CZECH TECHNICAL UNIVERSITY IN PRAGUE
FACULTY OF ELECTRICAL ENGINEERING
Technická 2, 166 27 Prague 6

BACHELOR THESIS

Georgios Ioannis Papaioannou
Diagnostics of crystalline silicon photovoltaic modules

Department of Electrotechnology

Supervisor of the bachelor thesis: Ing. Ladislava Černá

Study programme: Applied Electrical Engineering

Prague 2015

Solemn declaration

I declare that I carried out this bachelor thesis independently, and only with the cited sources, literature and other professional sources.

I understand that my work relates to the rights and obligations under the Act No. 121/2000 Coll., the Copyright Act, as amended, in particular the fact that the Czech Technical University in Prague has the right to conclude a license agreement on the use of this work as a school work pursuant to Section 60 paragraph 1 of the Copyright Act.

In Prague on 18th May 2015 . . . .

Georgios Ioannis Papaioannou

ACKNOWLEDGEMENT

Czech Technical University in Prague
Faculty of Electrical Engineering

Department of Electrotechnology

BACHELOR PROJECT ASSIGNMENT

Student: **Papaioannou Georgios- Ioannis**

Study programme: Electrical Engineering, Power Engineering and Management
Specialisation: Applied Electrical Engineering

Title of Bachelor Project: **Diagnostics of crystalline silicon photovoltaic modules**

Guidelines:

1) Process and describe the problematic of PV modules diagnostics with focus on Impedance Spectroscopy, Electroluminescence and Flash test measurement methods.
2) Apply the methods mentioned above on the set of crystalline silicon PV modules.
3) Discuss the results in terms of comparing results.

Bibliography/Sources:

[1] Gray, Jeffery L. The Physics of the Solar Cell. A. Luque a S. Hegedus. Handbook of Photovoltaic Science and Engineering. Chichester : John Wiley & Sons, Ltd., 2003, 3.
[2] CHEVNIDHYA, D., K. KIRTIKARA a C. JIVACATE Dynamic Impedance Characterization of Solar Cells and PV Modules Based on Frequency and Time Domain Analyses. Trends In Solar Energy Research. Hough, T.P. New York: Nova Science Publishers, 2006, s. 21-45. ISBN 1-59454-866-8; LCCN: 2005034740.
[3] Taylor, N. (Ed.): Guidelinesfor PV PowerMeasurement in Industry. Italy: EuropeanComission, Joint Research Centre, Institute forEnergy. 2010-04. Cite 2011. ISBN: 978-92-79-15780-6.

Bachelor Project Supervisor: Ing. Ladislava Černá

Valid until the end of the summer semester of academic year 2015/2016

L.S.

Ing. Karel Dušek, Ph.D.
Head of Department
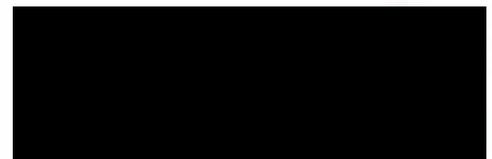
prof. Ing. Pavel Ripka, CSc.
Dean

Prague, March 25, 2015

CONTENTS

1 ABSTRACT

This thesis deals with the problematic of diagnostics of photovoltaic (PV) modules. Main used technologies and parameters are described with the focus on PV modules configuration. For measurement, there were three different measurement methods used – Flash Test, Electroluminescence test and Impedance Spectroscopy. All three methods are described and applied on the set of monocrystalline and multicrystalline PV modules. The results of single methods and their comparison are discussed.

KEYWORDS: *photovoltaics, flash test, electroluminescence, impedance spectroscopy*

Tato práce se zabývá problematikou diagnostiky fotovoltaických (PV) modulů. Jsou zde popsány hlavní používané technologie a jejich parametry se zaměřením na zapojení PV modulů. Pro měření byly použity tři metody – flash test, elektroluminiscenční test a impedanční spektroskopie. Všechny tři metody jsou popsány a následně použity pro měření série monokrystalických a multikrystalických PV modulů. Výsledky měření jednotlivými metodami I jejich vzájemné porovnání je uvedeno v závěru.

KLÍČOVÁ SLOVA: *fotovoltaika, flash test, elektroluminiscence, impedanční spektroskopie*

2   INTRODUCTION

The amount of sunlight hitting the earth's atmosphere continuously is $1.75 \cdot 10^5$ TW. However, only $1.05 \cdot 10^5$ TW comes to the earth's surface, because of atmospheric cloud cover transmittance. It is estimated, that if the irradiance on only 1% of the earth's surface could be converted into electric energy, with an efficiency of 10%, it could provide 105TW, whereas the total global energy needs are 25-30 TW for 2050. The global needs for electricity are increasing in fast pace nowadays, especially in developing countries, and the traditional oil fuels are becoming more and more expensive. On the other side, renewable energy sources are becoming more and more popular, not only because of their low CO_2 pollution, but also because the costs of some of the renewable energy technologies have decreased the last years. More specifically, the cost of PV modules have decreased rapidly the last years making PV technology one of the most promising renewable energy (RE) technologies [1].

Many materials are used for making PV cells and some of the most popular are: silicon, CdTe, GaAs, $CuIn(Ga)Se_2$, $CuInSe_2$ [2]. Generally, the PV cells are produced from light-absorbing materials and if the cell is illuminated, optically generated carriers produce an electric current when the cell is connected to a load.
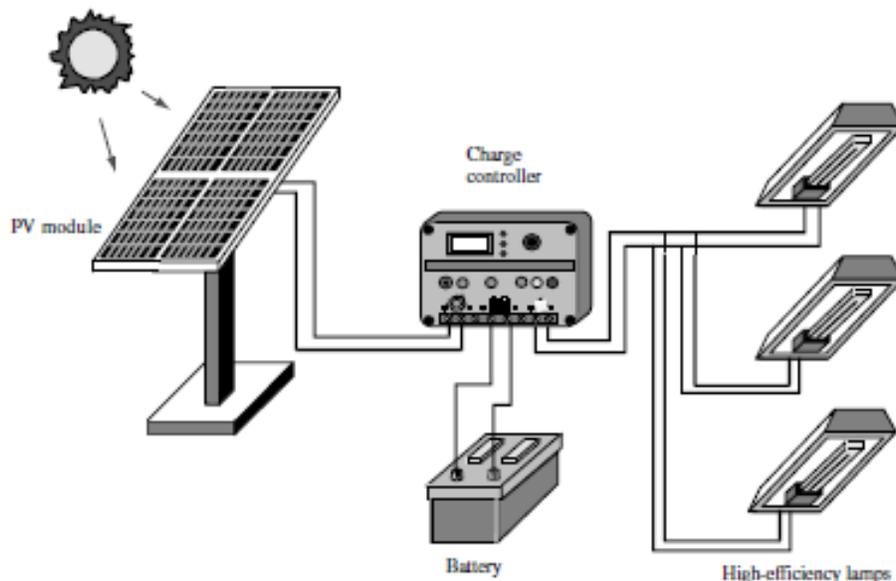

Figure1: PV system [3].

More specifically, solar radiation is made up of high-energy sub-atomic particles called photons. Each photon carries a quantity of energy (according to its wavelength) and some photons have more energy than others. When a photon of sufficient energy strikes a silicon atom in a solar cell, it moves the outermost silicon electron out of its orbit around the nucleus, freeing it to move. Free carriers, electron-hole pairs, must be separated to be used in the external circuit. In the case of PV cells, this is usually done by using the built-in electric field – PN junction. These carriers can be used for flowing through the load as a current. And as a result solar energy (in the form of photons) continuously generates electron-hole pairs that cause the electric current. More intense

sunlight gives a stronger current. Figure 4 proves it comparing I-V curves for different irradiances. More specifically, during the measurement a halogen bulb at specific distances from the PV cell emitted light and the basic parameters were recorded. The smaller the distance between the bulb (greater irradiance) and the PV cell, the stronger the current was produced.

Our focus is on crystalline silicon photovoltaic modules and their diagnostics applying Impedance spectroscopy, electroluminescence and flash test measurement methods. Saying diagnostics of c-Si we mean that we try to detect possible deviations against the specifications, check the performance against specifications, find a cause and asses the consequences.

There are the indoor measurements and outdoor measurements. Outdoor measurements may include temperature measurement and irradiance measurement but there is usually a problem achieving standard test conditions (STC) determining the nameplate values of PV modules and if it is possible a correction of the results is required and sometimes the error may be greater than 7 % [4], [5]. The STC combines the irradiation of a clear summer day, the cell/module temperature of a clear winter day and the solar spectrum of a clear spring day. More specifically the STC are 25 ˚C, 1 kW/m^{2}and AM 1.5 global spectrum [6]. STC help manufacturers and consumers to compare how different PV devices perform under the same conditions. The analysis of I-V characteristics at STC allows the determination of additional electrical performance parameters and helps to indicate the presence of parasitic resistances (series and shunt resistance). These measurement conditions do not represent real operating conditions of PV devices at the site of installation. Because of this, the instability of the results in outdoor measurements is a disadvantage. The reduction in efficiency can be caused by the variation in the amount of sunlight and the increase of operating temperature of the solar cell. Other parameters such as humidity or atmospheric turbidity can also affect the efficiency of the solar system. In general, the efficiency of a solar module, depends on its operating conditions and more specifically, researches have shown that the operating temperature of the cells is one of the most important parameters affecting the efficiency and power output meaning that increase of the cell temperature leads to decrease of the output (Figure 5).

For our case, we focus on indoor measurements and especially on flash tests (using the flash tester) for our measurements. An alternative for indoor measurements are the continual solar simulators usually used for measuring smaller areas than flash testers. Other methods used in the field is also thermography and nowadays electroluminescence which is still more laboratory method. Electroluminescence is basically a photographic measurement technique that helps researchers and scientists observe defects or inhomogeneities on the cells that cannot be seen by naked eye and may cause decrease in efficiency or output power. One of the omitted fact is that also AC parameters can be important because detailed analysis of AC parameters of solar cells can help researchers build more efficient PV systems. The main reason is that despite the fact that PV cells operate as DC devices, they exhibit complex impedance due to the solar cell physical structure. Changes of the temperature or irradiance make real part and imaginary part of the impedance of the cell change as well affecting the operation of the system. Furthermore, PV modules operate with inverters that have a working frequency in the range of kHz. AC parameters can than play the major role in the behavior of the system in the meaning of leakage currents. One of the methods that can be used for dynamic parameters determining is impedance spectroscopy, as using IS, the complex impedance $Z(\omega)=R(\omega) + jX(\omega)$ of a cell is measured directly in a large range of frequencies from 20Hz to 80000Hz.

3 THEORETICAL PART

3.1 Fundamentals of crystalline silicon PV cells

Crystalline silicon (c-Si) is silicon that has solidified into atoms arranged in crystal lattice and there are two types:

   a) monocrystalline silicon meaning silicon that has solidified into a single large crystal and
   b) polycrystalline or multicrystalline silicon meaning silicon that has solidified into many small crystalls in any orientation.

Crystalline silicon solar cells and modules both monocrystalline and polycrystalline have played a major role in PV industry, as the 85% of the market is constituted from c-Si and despite the new technologies coming to light, c-Si seems to dominate the market for next years [7]. The advantage of silicon is that it is abundant on earth's crust and the interest for this material began in 1960s, when scientists and researchers started using the chemical and electronic properties of Si. The silicon band gap is 1.12eV (in ambient room temperature) and it is an optimal value to make a good direct solar converter. The wafer thickness of silicon cells is currently about 150 μm and the efficiency has reached 25.6 % ± 0.5 % for Si(crystalline) and 20.8 % ± 0.6 for Si(multicrystalline) [8].

Figure 2: Left - polycrystalline solar cell, right - monocrystalline solar cell [3].

There are some basic parameters specifying a solar cell. They are:

Short-circuit current (I_{SC}): is the current in a short-circuited solar cell or module with output voltage 0 V.

Open-circuit voltage (V_{OC}): is the voltage obtained in open-circuit condition of solar cell or module

Fill Factor (FF): is obtained from the following equation and usually is the quality factor of PV cell (the maximum value for Si is 0.88 [9]):

$$FF = \frac{P_{\text{MAX}}}{V_{\text{OC}} \cdot I_{\text{SC}}} = \frac{I_{\text{MAX}} \cdot V_{\text{MAX}}}{V_{\text{OC}} \cdot I_{\text{SC}}} \tag{1}$$

Maximum power point (peak power) (MPP or P_{MAX}): the maximum power produced of the solar cell or module. It happens on I-V curve where $P_{\text{MAX}} = I_{\text{MAX}} \cdot V_{\text{MAX}}$, where I_{MAX} and V_{MAX} determine the optimal working point of the PV cell.

Series resistance (R_{S}): represents ohmic losses inside the cell

Shunt resistance (R_{SH}): represents defects, mainly shunts inside the structure of the cell (it is connected with the quality of the cell)

Solar cells are usually characterized according to their static characteristics which are open-circuit voltage (V_{OC}), short-circuit current (I_{SC}), voltage, current and power at maximum point (V_{MP}, I_{MP}, P_{MP}), the fill factor (*FF*), series-resistance (R_{S}) and shunt resistance (R_{SH}) measured under illumination or dark conditions. The series resistance, shunt resistance, fill factor and efficiency can be calculated from I-V curve and they can determine the performance of a PV cell or module. More specifically, low R_{S}, high R_{SH} and high *FF* means good quality PV cell. Also, I-V curve of a cell having high *FF* has rectangular-like shape and low *FF* has triangular-like shape. The dynamic parameters of solar cells however can be calculated by measurements when they operate under dynamic or transient conditions and another important parameters can be extracted by using these measurements: minority carrier lifetime, time constants, diffusion length, diffusion and transition capacitances (C_{D} and C_{T}).
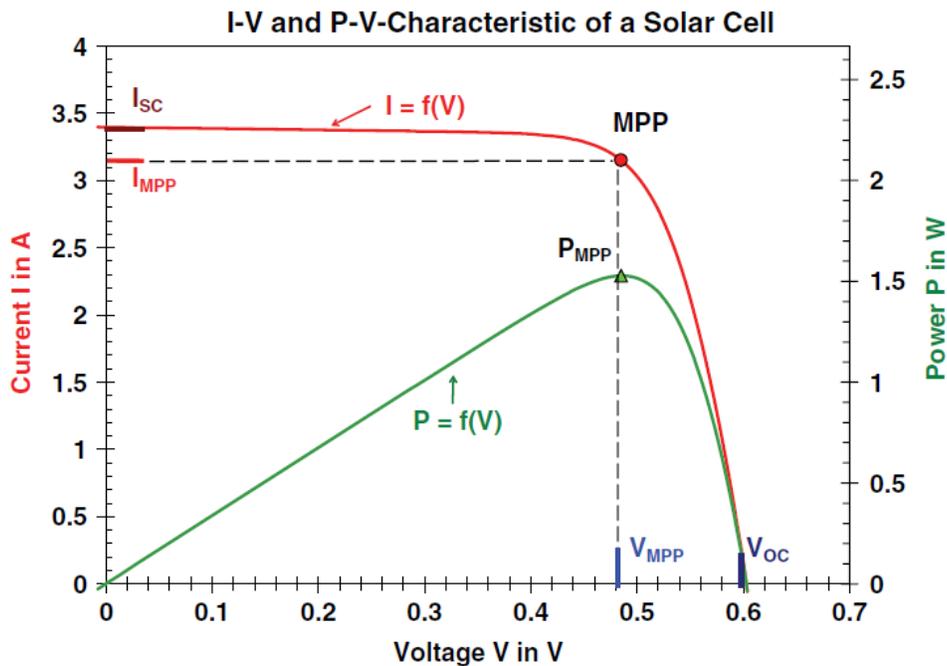

Figure 3: I-V curve and P-V curve of a monocrystalline silicon solar cell with a cell area of $102 cm^2$, irradiance G amounting to 1kW/m^2 and 25 degrees C [3].

The P_{MAX} can also be obtained:

$$P_{MAX} = V_{OC} \cdot I_{SC} \cdot FF \tag{2}$$

Solar Cell Efficiency (η$_{ec}$): can be obtained from equation:

$$\eta_{ec} = \frac{P_{MAX}}{P_{IN}} = \frac{I_{MAX} \cdot V_{MAX}}{incident\ solar\ radiation\ \cdot\ Area\ of\ solar\ cell} = \frac{V_{OC} \cdot I_{SC} \cdot FF}{G \cdot A_{C}} \tag{3}$$
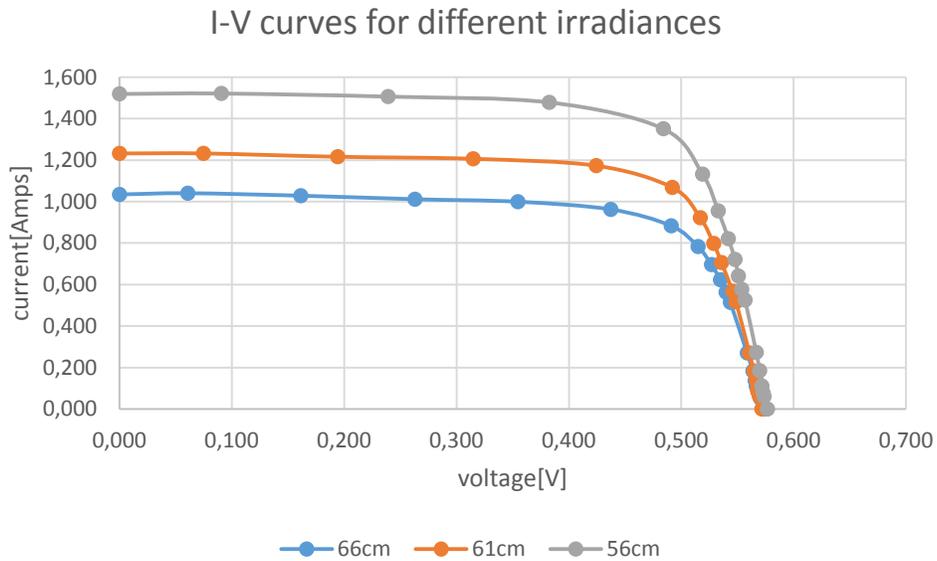

Figure 4: I-V curves for different irradiances.
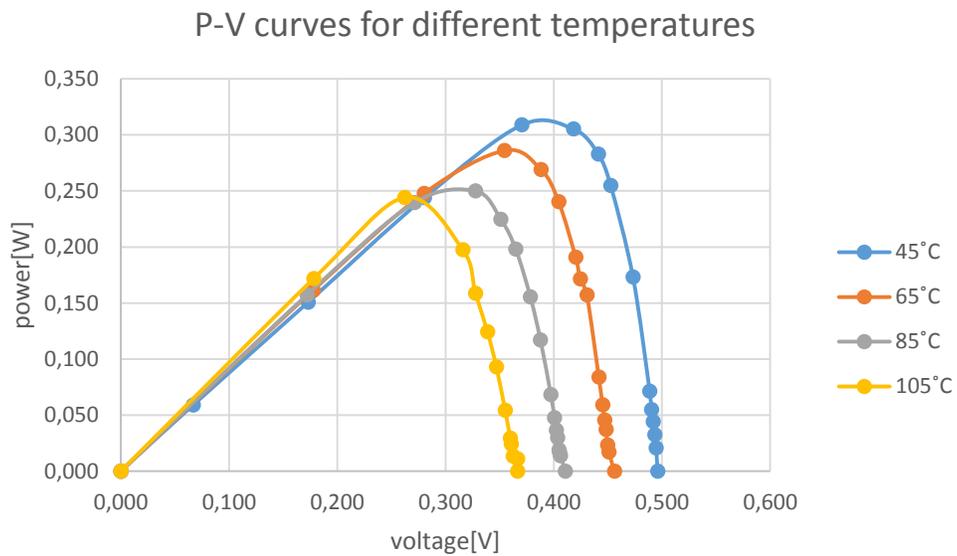
Figure 5: P-V curves for different temperatures.

3.2 Static PV cell model

Taking into consideration series and shunt resistances the following circuit is the equivalent circuit of a solar cell [2]:
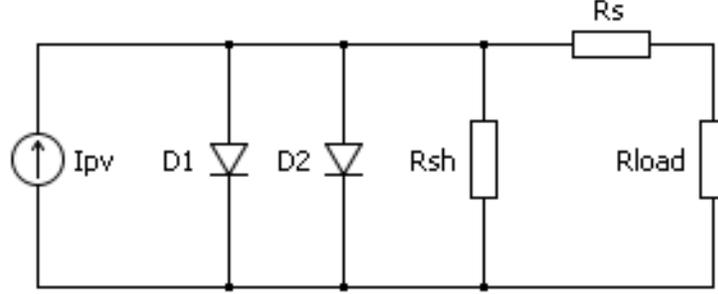

Figure 6: Equivalent circuit of solar cell.

where R_S is series resistance, R_{SH} shunt resistance and diodes are the representation of conductive mechanisms inside the PN junction. The equation describing it is [2]:

$$I = I_{PV} - I_D - I_{R_{SH}} = I_{PV} - I_{01}\left[\exp\left(\frac{eV_j}{\eta_1 kT}\right) - 1\right] - I_{02}\left[\exp\left(\frac{eV_j}{\eta_2 kT}\right) - 1\right] - \frac{V + R_s I}{R_{SH}} =$$

$$= I_{PV} - I_{01}\left\{\exp\left[\frac{e(V+R_S I)}{\eta_1 kT}\right] - 1\right\} - I_{02}\left\{\exp\left[\frac{e(V + R_S I)}{\eta_2 kT}\right] - 1\right\} - \frac{V + R_s I}{R_{SH}}$$

(4)

where:
I : current
I_{PV} : photocurrent = ideal solar cell short-circuit current I_{SC}
I_D : current flowing through the diode
V_j : voltage applied at the PN junction (diode)
V : voltage at the PV cell's terminals
e : elementary charge = $1.602 \cdot 10^{-19}$As
η : diode quality factor (1<n<2; close to 1 in most cases)
k : Boltzmann's constant = $1.38 \cdot 10^{-23}$J/K
T : absolute temperature (in K)
I_{01}: diffusion part of the current
I_{02}: generation-recombination part of the current

A simplification of the above equivalent circuit of solar cell is:
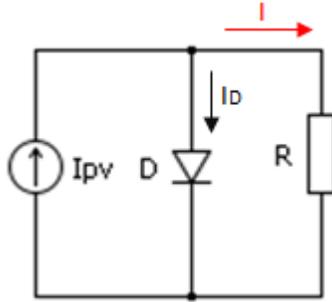
Figure 7: Simplified equivalent circuit of a PV cell.

and the equation describing it is:

$$I \;=\; I_{PV} - I_D \;=\; I_{PV} - I_S \left(e^{\frac{eV}{\eta kT}} - 1 \right) \;=\; I_{PV} - I_S \left(e^{\frac{eV}{V_T}} - 1 \right) \tag{5}$$

where:
I : current
I_{PV} : photocurrent = ideal solar cell short-circuit current I_{SC}
I_S : saturation current in the reverse direction
I_D : current flowing through the diode
V : voltage at the PV cell's terminals
e : elementary charge $= 1.602 \cdot 10^{-19}$As
η : diode quality factor (1<n<2; close to 1 in most cases)
k : Boltzmann's constant $= 1.38 \cdot 10^{-23}$J/K
T : absolute temperature (in K)

3.3 Dynamic PV cell model

In the case of AC solar cell model, transition capacitance (C_T) and diffusion capacitance (C_D) are added where C_T is the space charge capacitance of the depletion region and C_D is the capacitance due to minority carrier oscillation in response to AC signal.

A solar cell can be modeled by the following equivalent dynamic electrical circuit model:
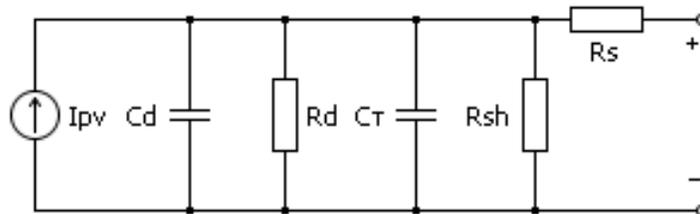

Figure 8: Dynamic equivalent circuit of a PV cell.

where:

I_{PV} = module current

R_S = series resistance due to the bulk resistance, wires and contacts

R_{SH} = shunt resistance

R_D = dynamic resistance of the diode

C_D = diffusion capacitance

C_T = transition capacitance

V_{ac} = dynamic voltage

ω = signal frequency

By combining C_D // C_T = C_P and R_D // R_{SH} = R_P, we get to the simplified dynamic model of the electric circuit of a PV cell, consisting of a resistor R_p and a capacitor C_p in series with a resistance R_S:
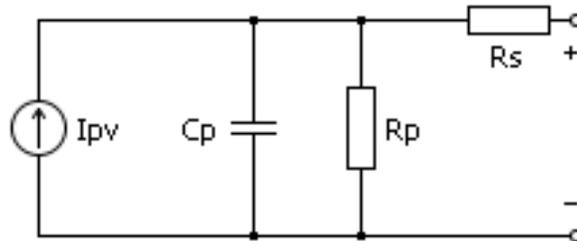
Figure 9: Simplified dynamic equivalent circuit of a PV cell.

where:

R_s = series resistance

R_P = parallel resistance

C_P = combined capacitance

3.4 PV module

PV cells can be connected in series, or in parallel to make a module. Connecting cells in series, the maximum power of each cell occurs at the same current and the total voltage is the sum of the voltages of each cell (Figure 10). Connecting cells in parallel, the maximum power of each cell occurs at the same voltage and the total current is the sum of the currents of each cell (Figure 11).
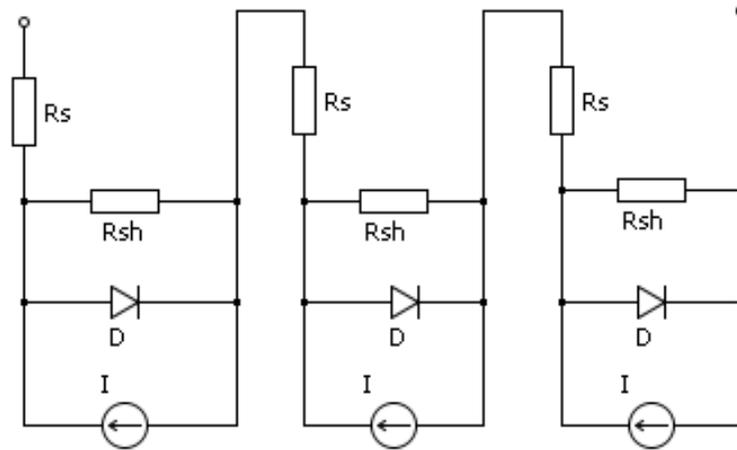
Figure 10: PV cells connected in series.
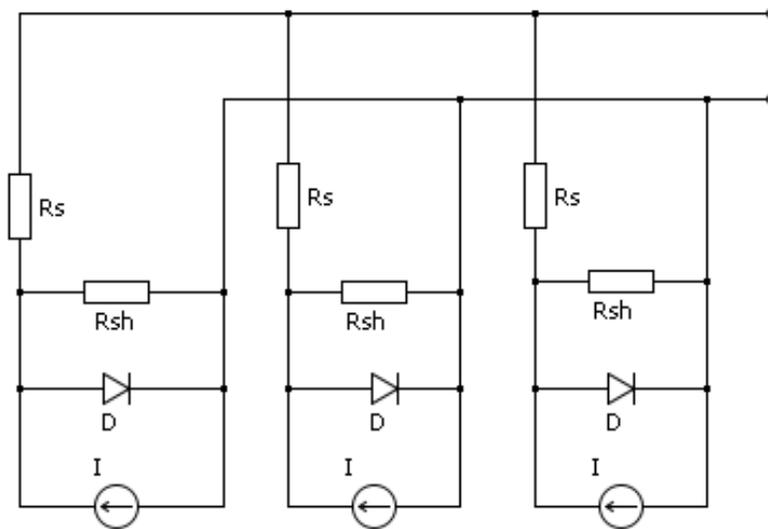
Figure 11: PV cells connected in parallel.
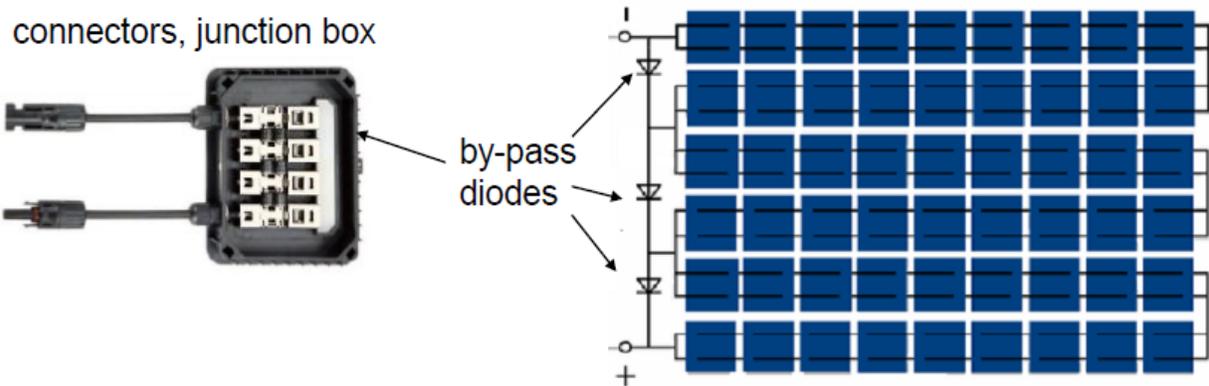
Figure 12: PV cells connected in series making a module.

In the previous figure, diodes are used to assure the efficiency of the PV module. More specifically bypass diodes are used across each string of cells, so if a cell fails the output power from the corresponding series connection will not be affected from the problematic cell.

Giving a more detailed example of series connection of two cells, we can suppose that one of them is problematic. In our case cell B is problematic and in such cases the current is determined by the problematic cell. The short circuit of the problematic cell B is half the current of cell A and comparing the I-V curves, it is obvious that the curve of cell A + cell B has the same character like the I-V curve of the cell B, instead of having cumulative character of summing cell A and cell B *MPP*'s.
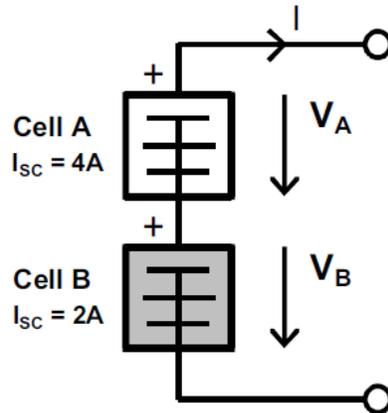

Figure 13: Two PV cells in series connection with problematic Cell B [3].
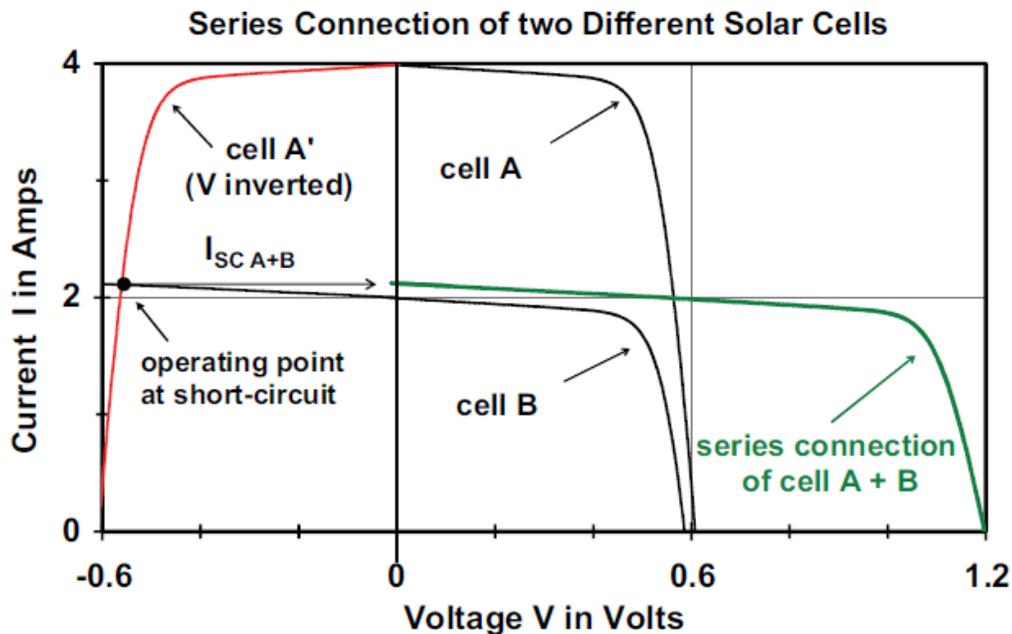

Figure 14: comparing I-V curves of cell A , problematic cell B and series connection A+B [3].
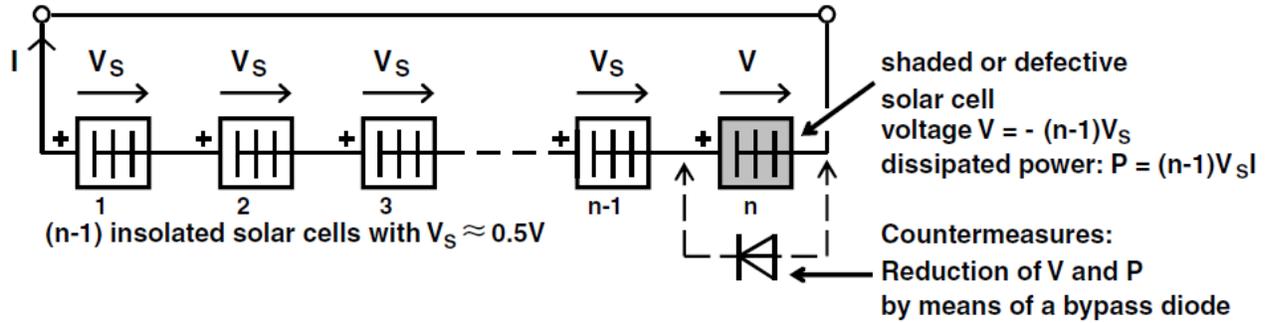
Figure 15: Using of bypass diode to countermeasure the effects from the problematic cell [3].

In the case the above scenario happens with more than two cells in series, it can cause overvoltage on the problematic cell and it can be avoided using bypass diode across the cells.

Using bypass diodes across each cell means that the cost is increasing rapidly and the solution is the use of one bypass diode for 12-24 series connected cells (Figure 16).
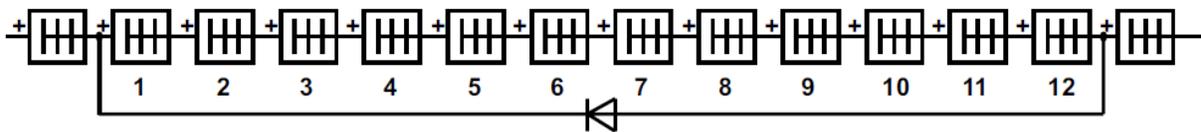
Figure 16: Using of one bypass diode for 12 series PV cell connection [3].

In the cases of up to12V systems where module short circuit does not happen, the avoidance of use of bypass diodes is possible, but for higher voltage installations, they must be protected by bypass diodes.

In the case of defective cell connected in parallel with other cells, the defective cell operates as a load absorbing the output from n-1 insolated cells (Figure 17). In similar way, the PV modules can be connected in series, parallel or combining series-parallel connections.
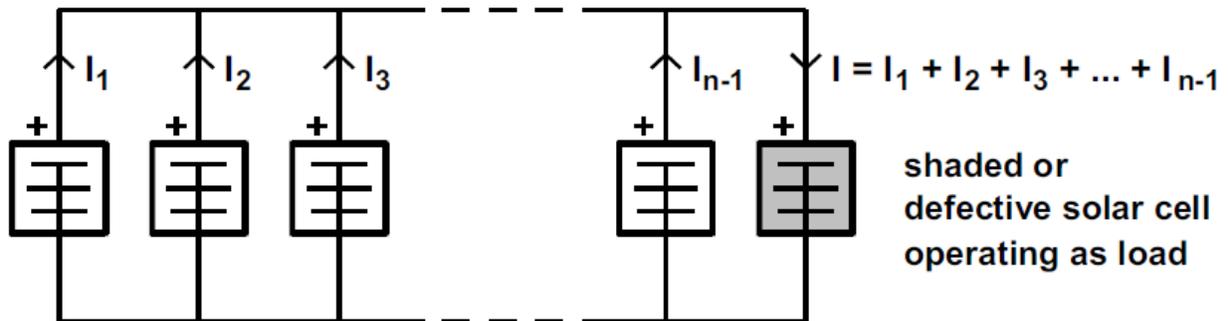
Figure 17: Situation with one defective PV cell in parallel connection [3].

3.5 The PV modules' string configuration

The Figure 18 shows a series connection of n modules, using bypass diodes across each module and blocking diode on either side of the series connection with some fusion or circuit breaker to prevent some anomaly of the system. For parallel connection of modules, it is important to note that only modules of same type (e.g. crystalline silicon) and with equivalent V_{OC} and V_{MPP} can be connected.

Principal Layout of a String consisting of several (n_{MS}) Solar Modules connected in Series

bypass diodes (unless already integrated in module)

string diode, blocking diode

isolation clamp, special connector

n_{MS} modules in series

if n_{SP}>3...4: Fuse, circuit breaker

Figure 18: Series connection of n modules [3].
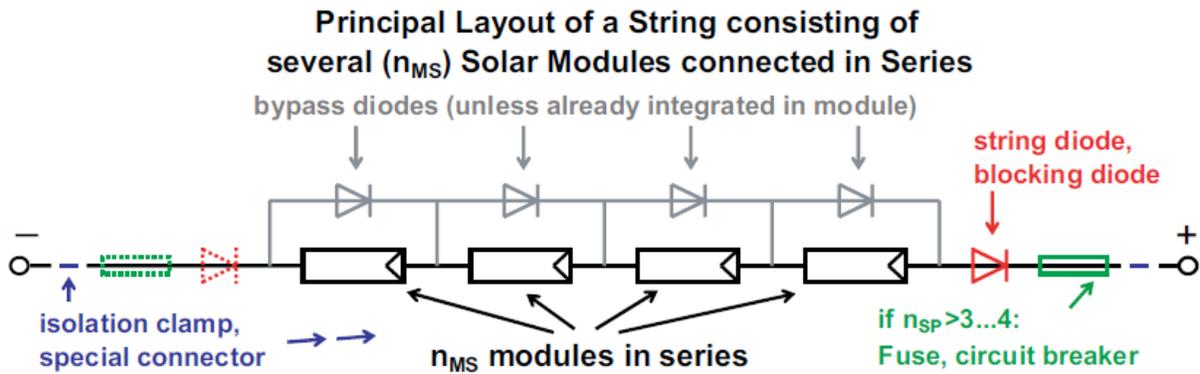
The Figure 19 shows a parallel connection of PV modules using fuses as a protection in malfunction case of the system and a large bypass diode in parallel to these series module-fuses groups which can conduct 1.25 times the aggregate short circuit current of all modules.

n_{MP} modules connected in parallel

large bypass diode

Figure 19: n modules connected in parallel [3].
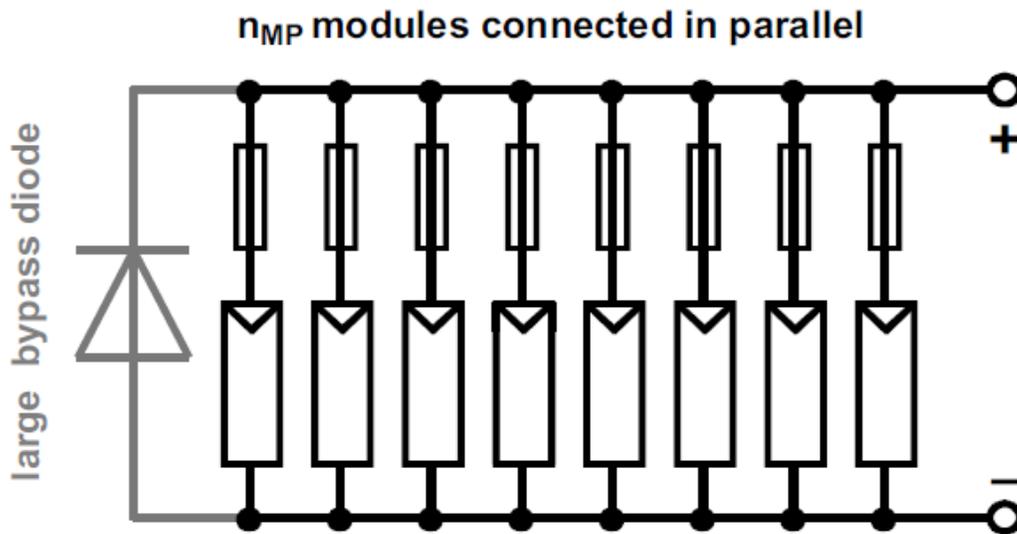
The scheme at the Figure 20 shows a parallel connection of series connected modules with protection against every possible failure of the system. Blocking diodes are used in each series connection and in case of diode failure, switch-brakers are used to protect the system.
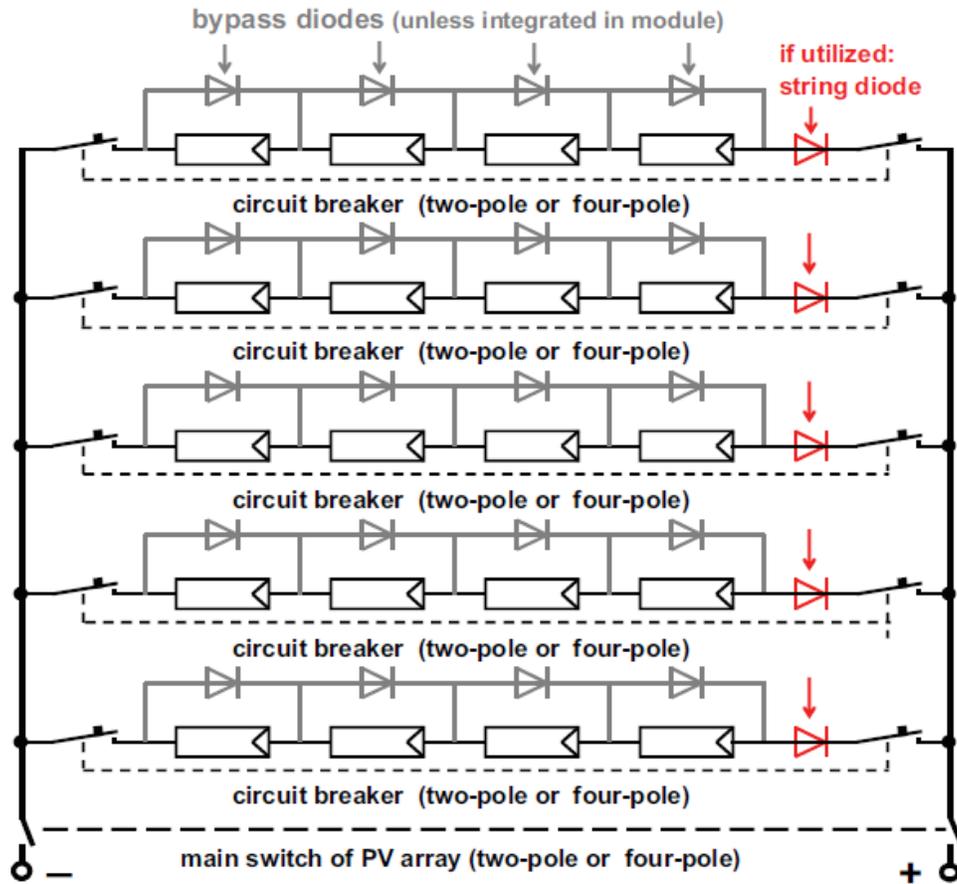
Figure 20: parallel connection of series connected modules [3].

3.5.1 Summary

The configuration of the PV module and PV system is very important factor which influences the behavior of the system and its parameters. I-V curves are deformed according to appropriate defects. In the following text are described the methods used for examining the building block of every PV system – PV modules.

3.6 Measurement methods

3.6.1 Impedance spectroscopy

Impedance spectroscopy is a method for investigating the properties and quality of solar cells by researchers explaining their fundamental mechanisms of operations. Impedance spectroscopy relates to electrochemistry helping investigate the charge transfers between solid conductor and an electrolyte. In case of solar cells, impedance spectroscopy techniques help evaluate the energy levels of majority carrier traps (in general, all those that cross the Fermi level).Using these methods, we can also get data for frequency dispersion and make better conclusions for the

system. Impedance spectroscopy is applied in systems with electrical contacts and is $Z(\omega)$ $= \dfrac{V(\omega)}{I(\omega)}$, where $V(\omega)$ ac voltage and $I(\omega)$ ac current at a frequency ω.

During impedance spectroscopy, the system is in steady state, and the impedance $Z(\omega)$ is measured getting the frequency values $f = \dfrac{\omega}{2\pi}$ from mHz to 10 MHz with 5-10 measurements per decade. It is important to verify the steady state of the system during measurement because changes of steady state can cause changes in impedance parameters (resistance, capacitance), and even temperature changes could cause changes in parameters. During each steady state, detailed record of information values is necessary, and it makes the measurement quite time-consuming. But getting information of frequency and recording the values, it makes it possible to observe the dynamic properties of the system. The following scheme shows the way impedance spectroscopy technique is used:
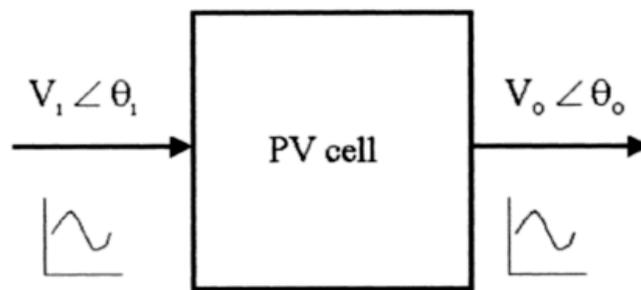

Figure 21: Representation of the IS [10].

A new idea is applying sinusoidal signals as inputs with varying frequencies and superimposing on the DC bias in the dark in forward bias and in reverse bias conditions, the impedances of the PV cell are measured and it makes it possible to plot the impedance loci. There is also a new alternative impedance measurement technique for PV cells, where square wave inputs are used as inputs superimposed on a DC biasing voltage in either forward or reverse condition. The advantage of this new method is that one whole impedance locus can be measured by using 2-3 square wave inputs at different frequencies in comparison to the previous method which needs more steps and time. It makes the measurement less time-consuming, simpler but also less expensive using only basic instruments like oscilloscope and signal generator. The Figure 22 compares the two impedance measurement techniques and shows that the results are similar.

Measuring the dynamic impedance of solar cells and plot them in the complex plane, it is possible to understand about the quality of the cell even if the static characteristics of the cell are unknown. More specifically low R_S and high R_{SH} are cells of good quality than those ones having high R_S and low R_{SH}, which are of low quality. The Figures 23 and 24 compare two PV cells, one of good quality and one of bad quality, using both the static characteristics and the impedance characteristics of the cells. M1 being of good quality and M2 being of low quality making us remind that good quality PV cells have rectangular-like shape because of high FF and bad quality PV cells have triangular-like shape because of low FF.

16
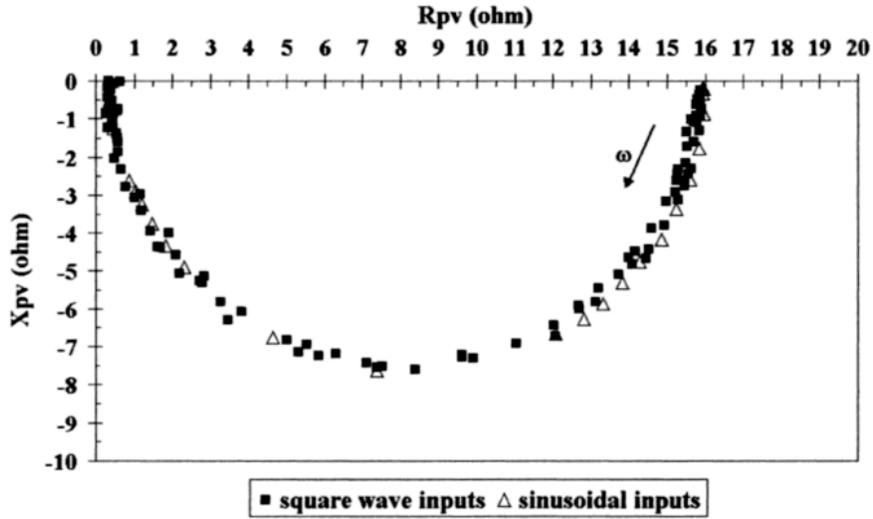
Figure 22: Comparison of impedance loci measurement using square wave inputs and sinusoidal inputs at forward biasing level of 0.2V [10].
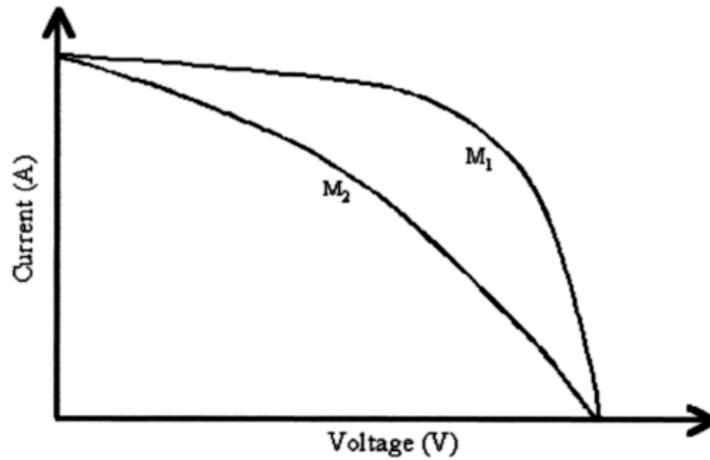

Figure 23: Comparison of M1 and M2 cells using static characteristics. [10].
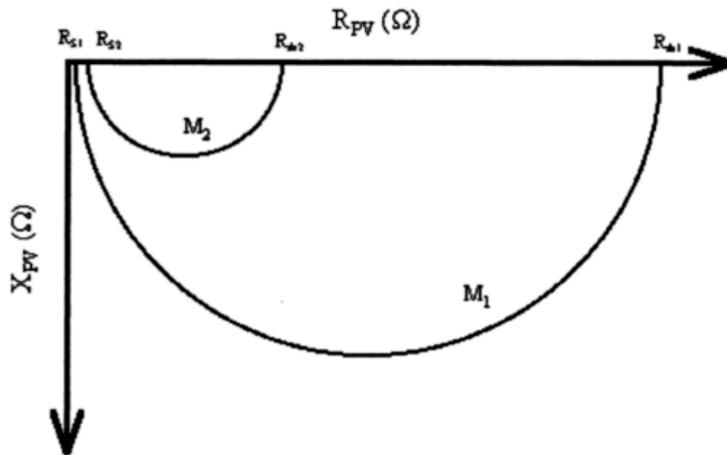
Figure 24: Comparison of M1 and M2 cells using impedance characteristics. [10].

17

In terrestrial applications, the PV systems may operate in temperatures ranging from 10˚C to 50˚C. Changes in temperature affect the efficiency and the operation of the system. Analyzing the AC parameters of a PV system and studying their behavior in changes of their environment help scientists build more reliable and efficient PV systems. In this case impedance spectroscopy seems to be a very useful tool for cells characterization. More specifically, impedance spectroscopy is characterized by the measurement and analysis of some or all impedance related functions. The complex impedance $Z(\omega) = R(\omega) + jX(\omega)$ from the system is measured in a large range of frequency where $R(\omega)$ is the real part of $Z(\omega)$ and $X(\omega)$ is the imaginary part of $Z(\omega)$. A pure sinusoidal voltage in different frequencies is applied to the system under test and the phase shift and amplitude of the voltage and current are measured. The ratio between the applied voltage and resultant current is calculated and this is the impedance of the device under test. If we plot the real and imaginary values $R(\omega)$ and $X(\omega)$ we measured on complex plane in dependence of frequency, we take the impedance spectrum of the system.

From the resulting plot, other equivalent circuit parameters can be further calculated. The following figure shows the relationship between the imaginary part $X(\omega)$ and the real part $R(\omega)$ of the complex impedance. The result is semicircles and a simple observation could be that the semicircles are smaller with increase of temperature. This indicates that the conductivity of the measured cells increase with increase of temperature – parasitic shunt resistance becomes more dominant (Table 1 and Figure 25). For this specific plot, we could also conclude that because the centers of the semicircles are below the real axis $R(\omega)$, the AC equivalent circuit of the PV cell is a leakage resistance R_{SH} connected in parallel with capacitance C_p with a single time constant and this parallel connection is connected in series with series (bulk) resistance R_S (Figure 26).
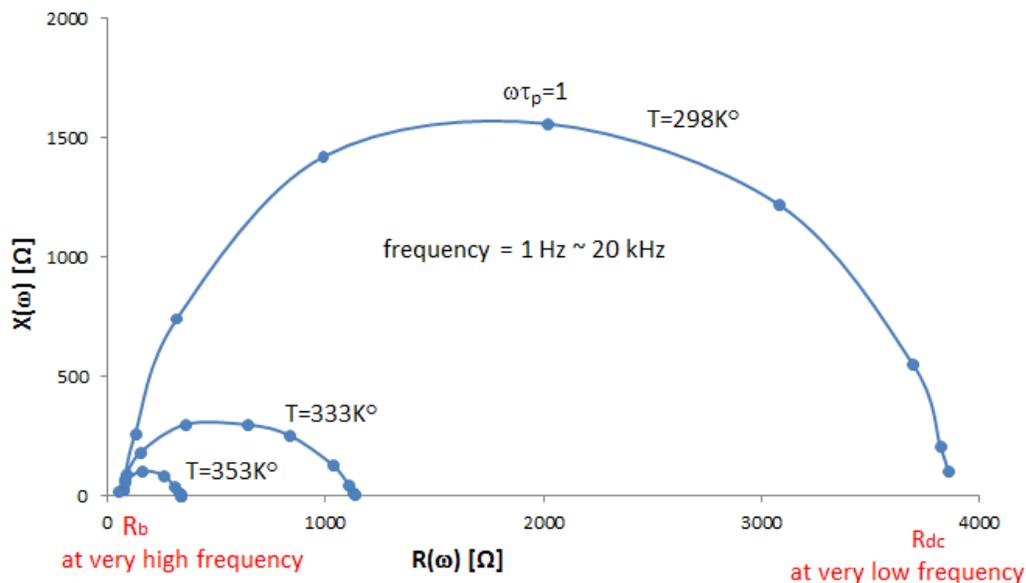
Figure 25: Impedance spectra of the multicrystalline silicon solar cell at different temperatures. [11].
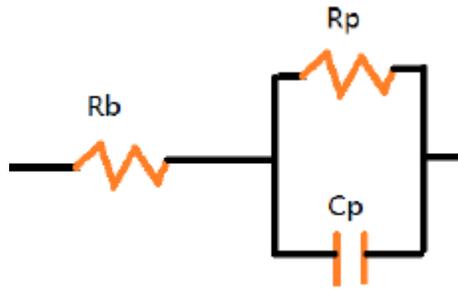
Figure 26: The equivalent circuit for the crystalline silicon PV cell [11]

Table 1: Calculated values of solar cell AC for different temperature [11]

T_F (K)	298	333	353
$R(\omega)$ (KΩ)	3.861	1.135	0.34
$X(\omega)$ (KΩ)	1.56	0.3	0.104
f (Hz)	81	600	2230
C_p (nF)	1260	885	687
τ_p (µS)	1970	265	71.4
R_P (KΩ)	1.56	0.3	0.104
β	0.1	0.163	0.2

Another conclusion from this measurement example is that capacitance decreases as frequency increases.

3.6.1.1 Diagrams for different RC combination

For understanding the obtained graphs is useful to know these diagrams for various RLC configuration:

Series R_1C_1:

$$Z(\omega) = R_1 + \frac{1}{j\omega C_1} \tag{6}$$
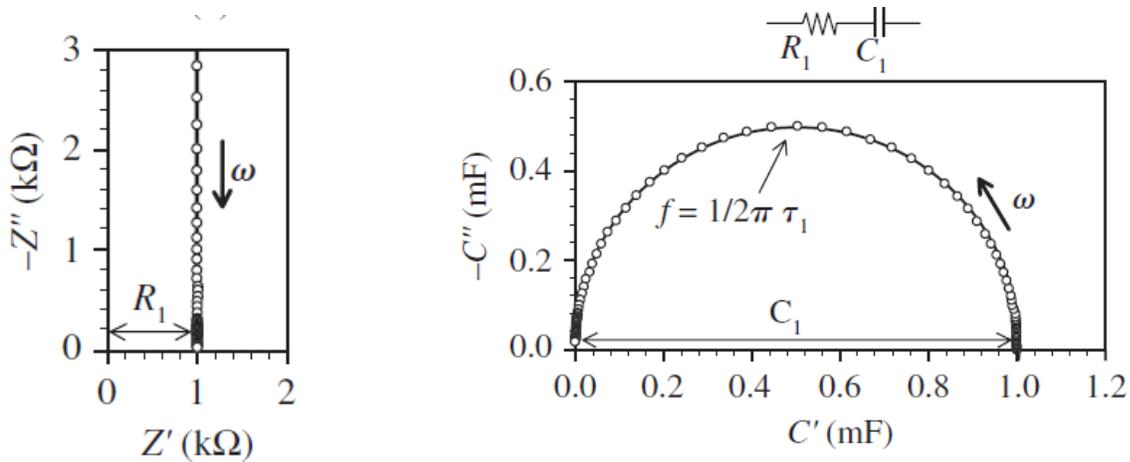
Figure 27: Representation of impedance of equivalent circuit R1=1kΩ, C1 = 1mF, τ1 = 1s.The arrow indicates the direction of an increasing angular frequency ω [12].

Parallel $R_1\|C_1$ with series R_2

$$Z(\omega) = R_2 + Y_1 = R_2 + \frac{R_1}{1 + R_1 j\omega C_1} = R_2 + \frac{R_1}{1 + j\omega\tau_1} \tag{7}$$
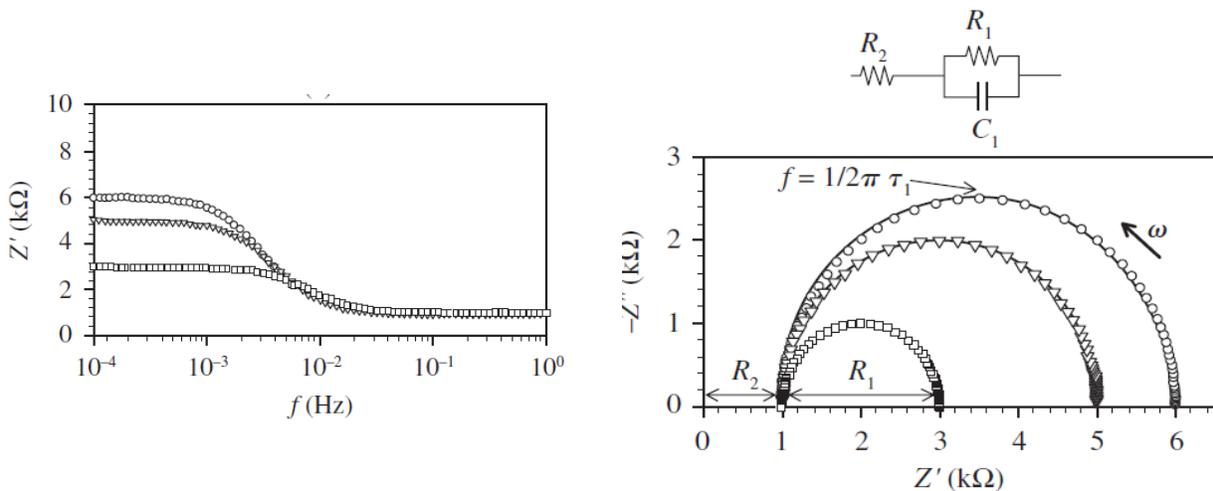
Figure 28: Representation of the impedance of an equivalent circuit, R1 = 5, 4, 2 kΩ, C1 = 10mF, R2 = 1kΩ. [12].

Parallel connection of two series RC

$$Z(\omega) = R_1 + \frac{1}{j\omega C_1} || R_2 + \frac{1}{j\omega C_2} = \frac{j\omega(\tau_1 + \tau_2) + 1 - \tau_1\tau_2\omega^2}{j\omega(C_1 + C_2) - \omega^2(\tau_1 C_2 + \tau_2 C_1)} \tag{8}$$
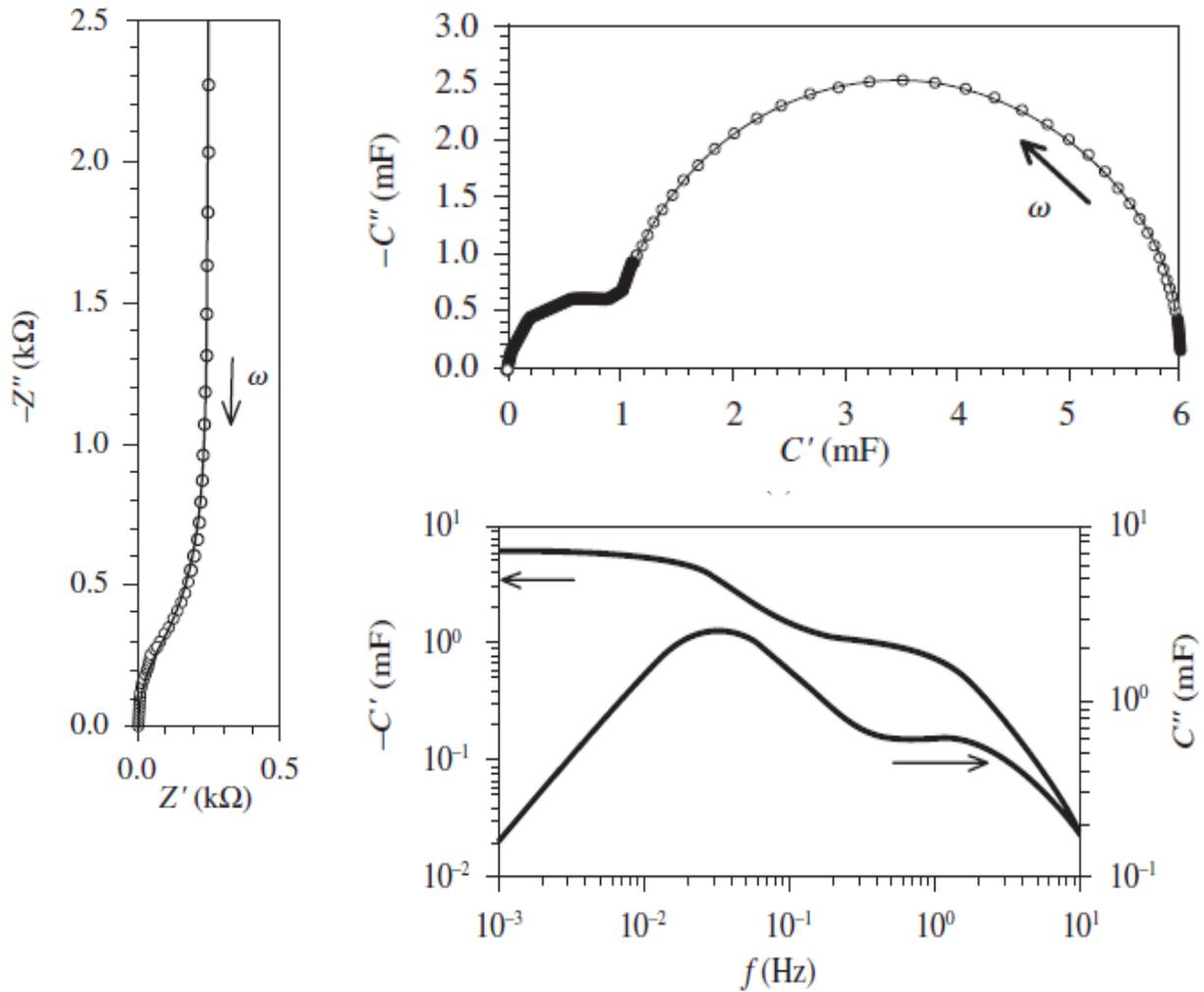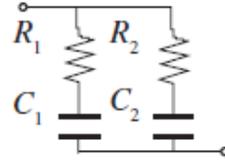
Figure 29: Representations of the impedance of equivalent circuit R1 = 1kΩ, C1=5mF, τ1=5s, R2=0.1kΩ, C2=1mF, τ2 =0.1s. [12].

Parallel R||RL||C combination

$$Y(\omega) = \frac{1}{R_1} + \frac{1}{R_3 - j\omega L_3} + j\omega C_1 \qquad (9)$$
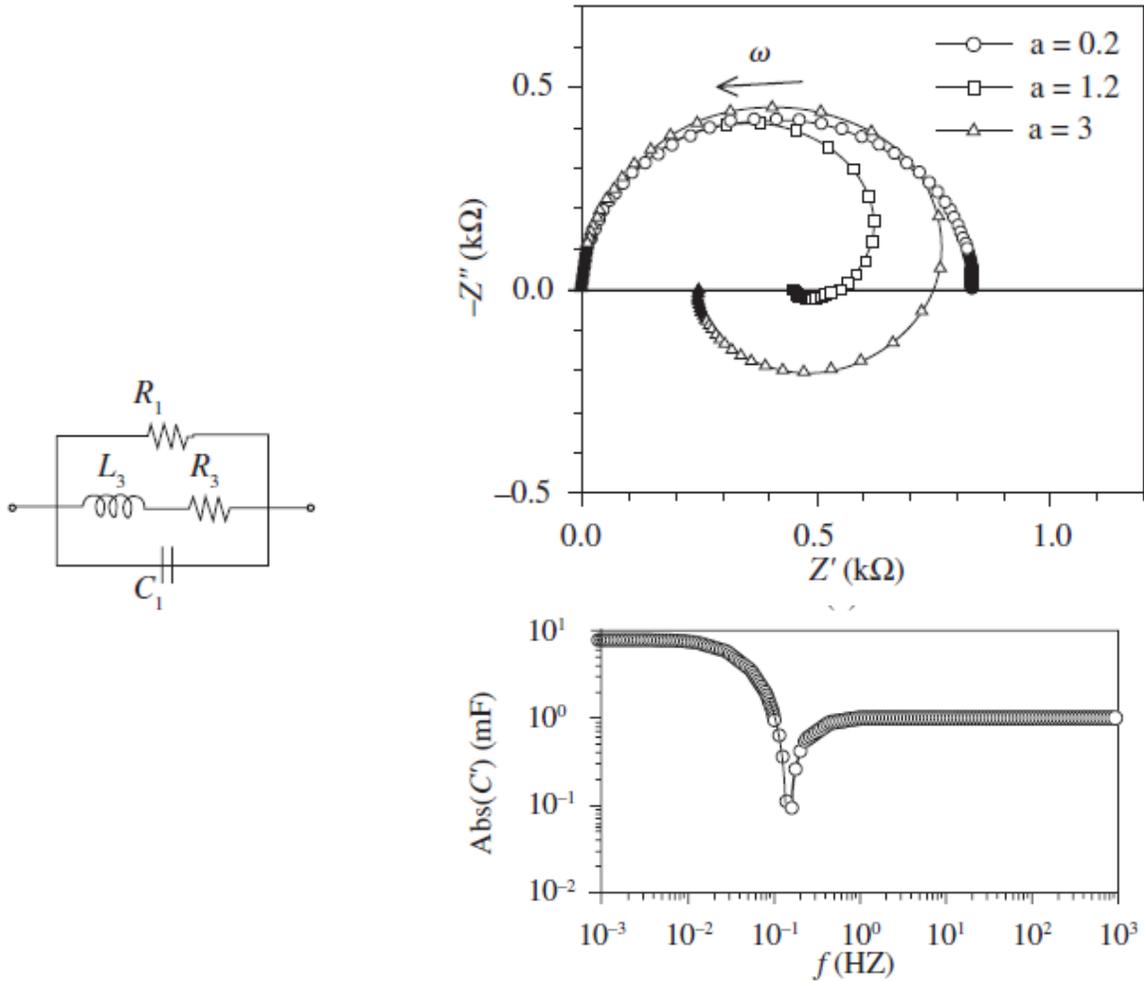
Figure 30: Representation of the impedance of equivalent circuit R1=1kΩ, C1=mF, L3=1kHz , R3 = R1/α , α varies as shown. [12].

3.6.1.2 *Summary*

From IS method we can establish the other parasitic parameters which manifestations cause specific distortion of the measured curve (observable at previous Figures number 27, 28, 29 and 30).

3.6.2 Electroluminescence (EL)

Electroluminescence (EL) is a photographic technique which is used under forward bias as a diagnostic tool for defects on PV cells and modules. More specifically, the cells emit infrared light (wavelength from 1000 nm to 1200 nm) whose intensity reflects the number of minority carriers in base layers. In this way, possible cracks and breakages can be detected and the electronic materials of the cell can be analyzed more thoroughly using developed techniques related to absorption of near bandgap light and local series-resistance. A Si CCD camera is usually used capturing an area of 1 cm – 1.5 cm in less than 1 s. The temperature of the cell plays also an important role, because changes in temperature (from 25 °C to 100 °C) leads to different EL intensity contrasts and it can help for further analysis of the results. This fast and reliable technique is used in large scale production of solar cells and modules for evaluating the quality and acquire as high efficiency as possible.
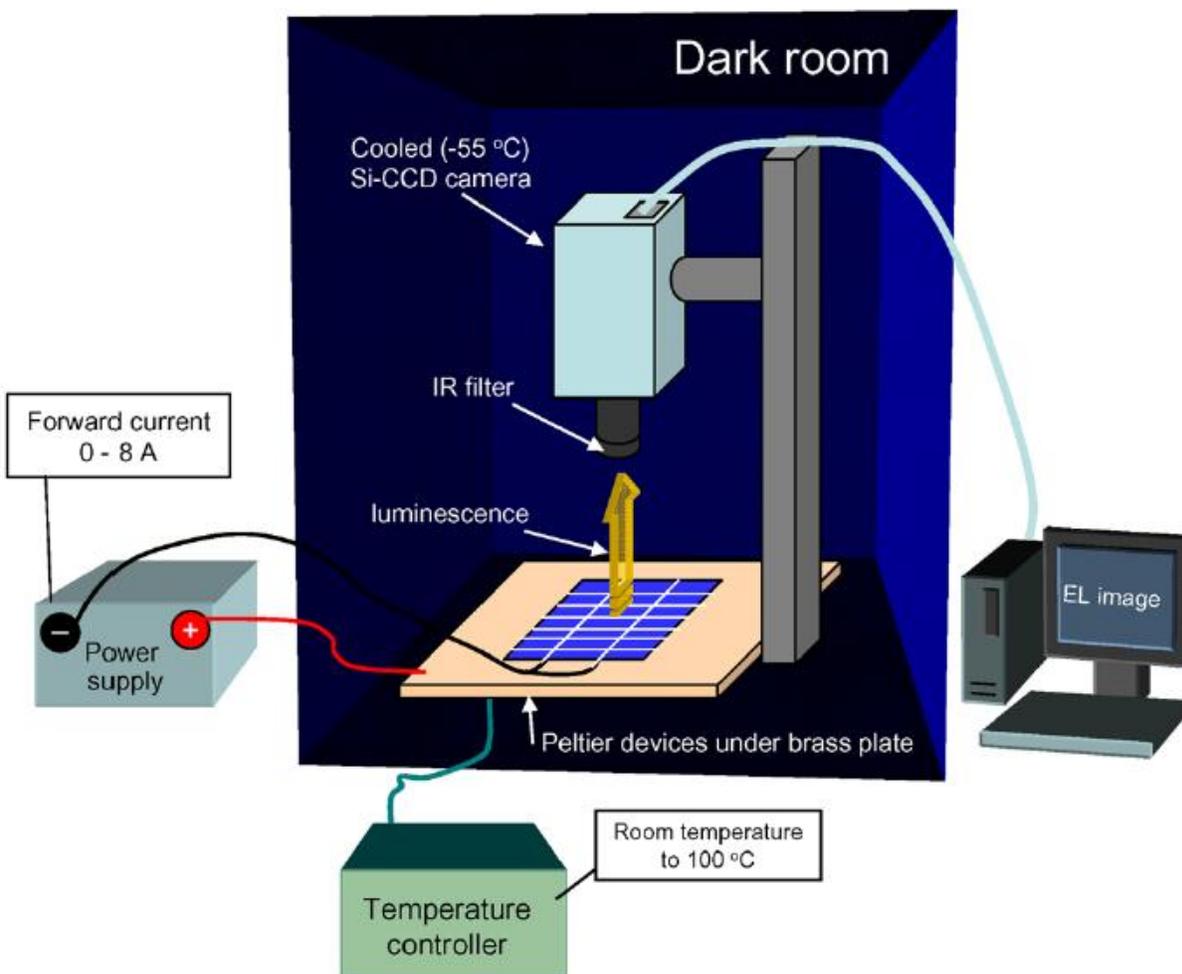
Figure 31: EL technique. [13]

In the figure below, and having used EL technique for a multicrystalline Si solar cell, we can observe the inhomogeneities that are impossible to be observed with a naked eye.
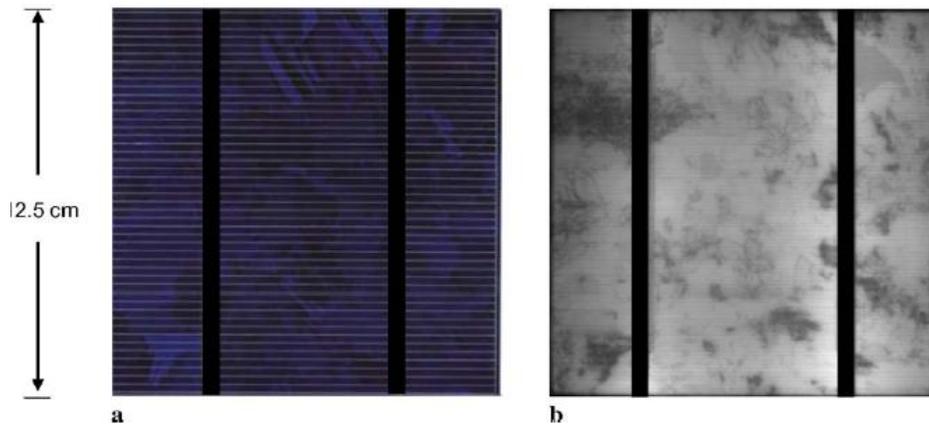
Figure 32: Comparing the pictures of a multicrystalline Si solar cell with and without EL [13].

As was mentioned previously, the change in temperature is crucial because the temperature has a larger effect on the intrinsic deficiency (crystallographic defects) than the extrinsic deficiency (wafer breakage). Comparing the EL images from different temperatures, it is possible to see the points which were more affected by the change of temperature. As an example, the figures below shows the EL pictures at 25 degrees, 100 degrees and the subtracted picture where the whiter points are the points affected more by the temperature change. EL combined with other techniques can improve the quality and efficiency of the PV cells and modules.
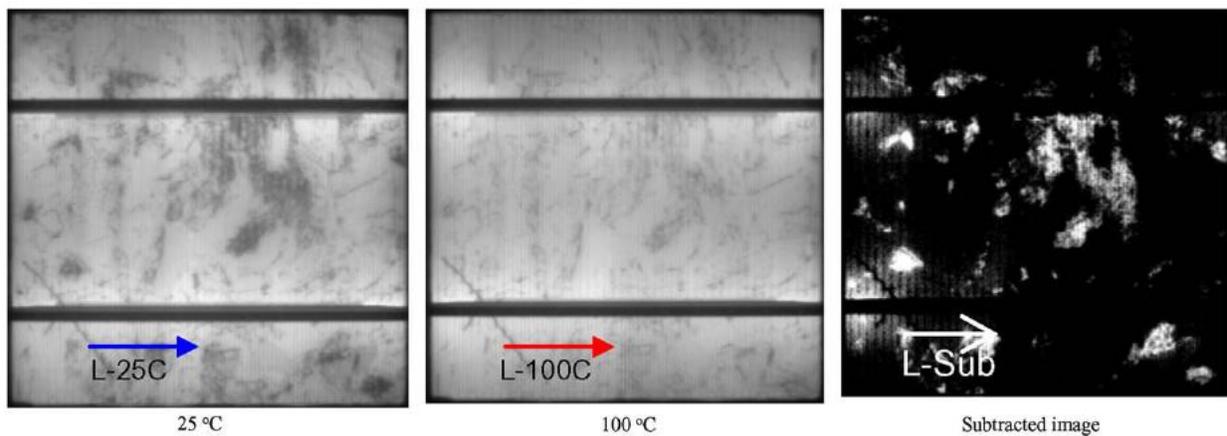
Figure 33: Comparing EL pictures from different temperatures and the result from subtracting the pictures [13].

3.6.3 Flash Tests

Flash testers are used for measuring solar cells and modules but usually they are expensive and susceptible to errors. The great advantage of flash testers over continuous illumination testers is that flash testers provide high light intensity with good uniformity over large areas and the short time pulse of light causes little heating of the cell. There are two main types of flash testers: the single flash and multi-flash. The most of commercial systems are single flash.

Single flash testers emit a constant light intensity which lasts for few milliseconds and during this time the I-V curve is recorded. This method is expensive because of the high power outputs of the flashes, usually tens of kilowatts. These high power flows makes their regulation difficult from circuits point of view and also the little time of duration for I-V curve shaping requires a high speed electronic load for the cell and transient errors are possible to happen.

Multi flash systems differ from single flash testers that they use many flashes for recording the I-V curve and each flash record just one point of the I-V curve. For this reason, they are cheaper and simpler than single flash testers, as they don't require high-speed load and they don't require regulation of the flash. And also they are less vulnerable to transient errors.

Constant-voltage flash testers is another method for measuring solar cells which is less sensitive to transient errors than other flash tester methods since it maintains a nearly constant bias voltage during each flash. Another advantage of this method is that it shapes a family of I-V curves over a decade range of light intensity which gives more data for cell performance. This family of I-V curves can give information about the behavior of the cell in different light intensities. This method is used especially for concentrator cells and 1-sun cells.

As was stated previously, measurement errors often occur using flash testers because of transient effects. Transient errors are caused because of the rapid changes of the charge distribution in the cell. Minority carrier concentrations are much higher in forward bias than at short circuit, so large amounts of charge have to be moved when changing bias condition [14].

As a solution for eliminating the transient errors in case of single flash testers, the duration of the flash pulse could be extended if possible for the flash tube to handle the maximum pulse energy. In another way, someone could correct the errors either estimating the capacitance of the cell and recalculating the curve without it, or through dark I-V measurements. For multi-flash testers however, another solution could be applied. Since the transient error occurs because of rapid changes in bias voltage, keeping the voltage constant during each flash and changing it slowly between flashes could eliminate the errors. But keeping the voltage constant eliminates the transient errors in some extent but not entirely [15].
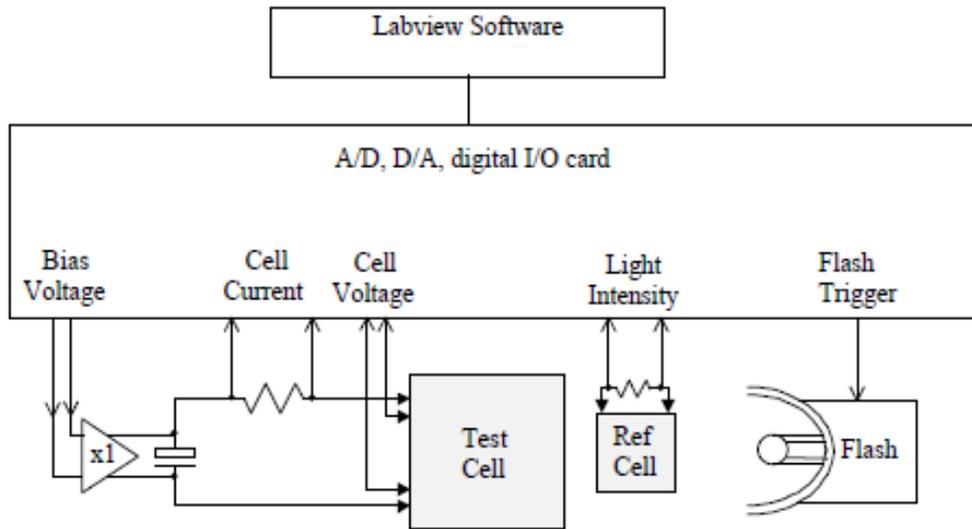
Figure 34: Block diagram of Flash Tester [14].

4   PRACTICAL PART

The scope of our measurements is the process and description of the problematics of PV modules diagnostics with focus on Impedance Spectroscopy, Electroluminescence and Flash test measurement methods and their comparison.

4.1   Measured objects

For our measurements we tested 18 PV modules in total, 9 of them are mono-crystalline and 9 of them are multi-crystalline. All 18 PV modules have the same characteristics:

Phono Solar
Module Type PS15(M)

Rated Power at STC	(Wp)	15	W
Rated Power Voltage	(Vm)	2.1	V
Rated Power Current	(Im)	7.5	A
Open Circuit Voltage	(Voc)	2.71	V
Short Circuit Current	(Isc)	8.04	A
Nominal Operation Cell Temp	(NOCT)	45˚C±2˚C	
Maximum Fuse Rating		10A	
Application Class		A	
Dimension		376x376mm	

4.2   Measurement devices

The device that was used for impedance spectroscopy measurement was: MCP TH2818 Automatic Component Analyzer (Figure 35).

Figure 35: During impedance spectroscopy measurement.

For electroluminescence measurements the following tester was used: GSolar GEL-M4 Solar Cell Module
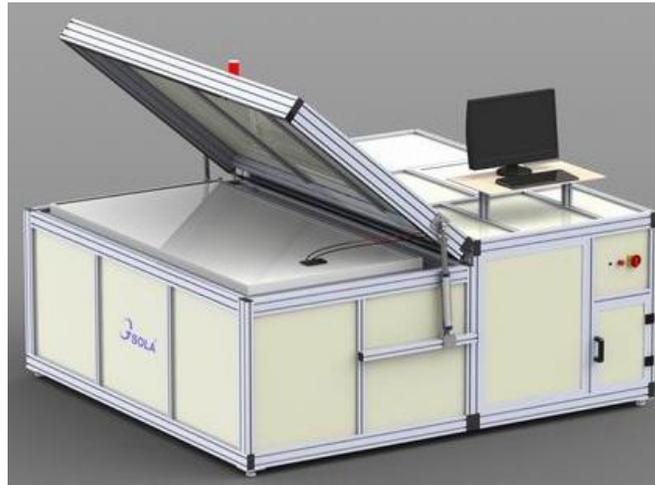
Figure 36: The electroluminescence tester was used.

For Flash Tests the following tester was used: Pasan SunSim 3c module tester. The equipment of Pasan's SunSim 3c module tester is composed of:

- the flash generator with separated box, which generates a pulse of calibrated light
- the electronic load (IV tracer) which scans the Device under Test (DuT) response on the full IV curve during the light pulse
- the monitor cell which allows to control and measure the effective light irradiance
- a PC with the measurement software

The Pasan SunSim 3c is mounted in a dedicated dark tunnel and the optical distance between the front of the flash box and the DuT is 5.5m.

Figure 37: The flash tester was used for our measurements.

4.3 Measured results

4.3.1 Electroluminescence:

After testing the 18 PV modules and getting the corresponding pictures, we display three of them: no6, no20, no16 (more pictures can be found in annex [B]):
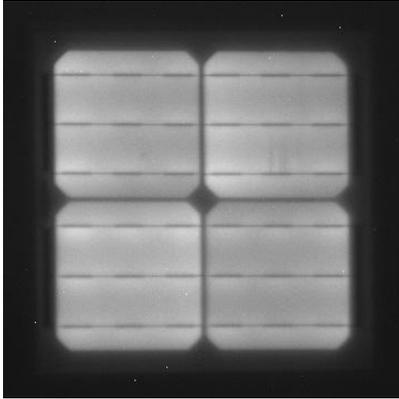
Figure 38: Mono-crystalline (no6).　　Figure 39: Multi-crystalline (no20).　　Figure 40: Multi-crystalline (no16).
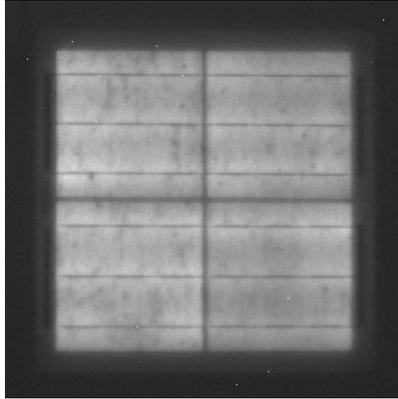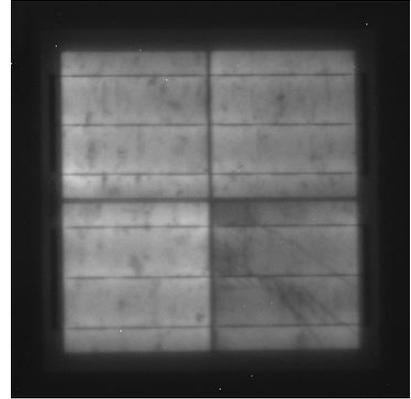
From the pictures above, and comparing with the other pictures of the PV modules, we can see that no6 is a typical mono-crystalline PV module without defects or microcracks. Comparing the pictures for multi-crystalline PV modules, no16 differs from the other multi-crystalline PV modules because of the defects on the down-right side of the module. Such a defect can decrease the efficiency of the module and cause problems to the system. However the decrease of the efficiency will be quite small because only the down-right cell seems to be defective, furthermore this defect seems to be in the small range for now. Comparing the pictures from mono-crystalline and multi-crystalline, we can see the differences between the structures of these two kinds of PV modules. Multi-crystalline modules have more inhomogeneities than mono-crystalline ones, however this kind of inhomogeneities do not affect the operation or the efficiency of the multi-crystalline modules.

4.3.2   Flash Test

After testing the modules on sun simulator and getting the results for each of them, we can compare the efficiency or other important parameters among the modules. The results for no6, no20 and no16 are the following (the rest can be found in annex[C]):

4.3.2.1   *Measurement of the module number 6:*

Producer:	Phonosolar	
Type:	PS15M	
Serial number:	6	
Designation in LPVS:		
Date of the measurement:	04-05-15	
Actual temperature:	24.0	°C
The values are converted to the temperature:	25.0	°C
$G =$	1.0	kW/m2
$I_{sc} =$	8.925	A
$V_{oc} =$	2.579	V
$\eta =$	11.59	%
FF $=$	71.18	%
$P_{MAX} =$	16.386	W
$V_{Pmax} =$	1.987	V
$I_{Pmax} =$	8.248	A
$R_s =$	0.0	Ω
$R_p =$	49.2	Ω
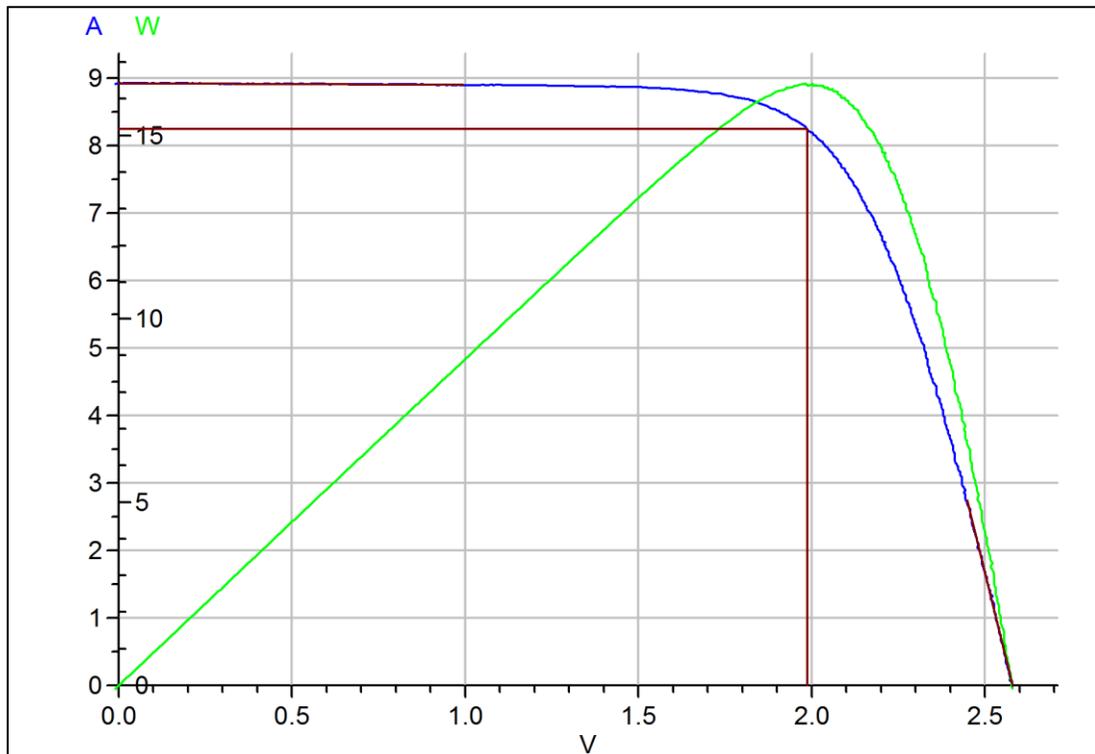
Figure 41: I-V and P-V diagrams for module no6.

4.3.2.2 Measurement of the module number 20

Producer:	Phonosolar	
Type:	PS15P	
Serial number:	20	
Designation in LPVS:		
Date of the measurement:	04-05-15	
Actual temperature:	23.8	°C
The values are converted to the temperature:	25.0	°C
$G =$	1.0	kW/m2
$I_{sc} =$	8.832	A
$V_{oc} =$	2.561	V
$\eta =$	11.31	%
FF =	70.72	%
$P_{MAX} =$	15.996	W
$V_{Pmax} =$	1.969	V
$I_{Pmax} =$	8.125	A
$R_s =$	0.0	Ω
$R_p =$	68.7	Ω
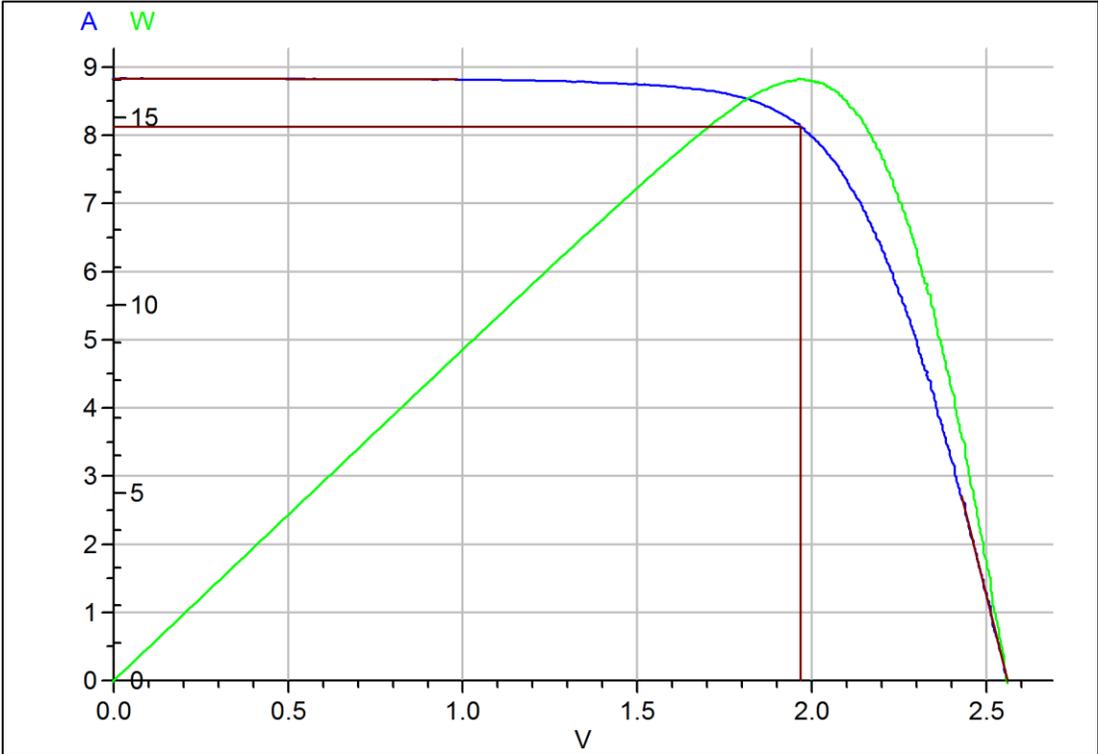
Figure 42: I-V and P-V diagrams for module no20.

4.3.2.3   Measurement of the module number 16

Producer:	Phonosolar	
Type:	PS15P	
Serial number:	16	
Designation in LPVS:		
Date of the measurement:	04-05-15	
Actual temperature:	23.8	°C
The values are converted to the temperature:	25.0	°C
$G =$	1.0	kW/m2
$I_{sc} =$	8.806	A
$V_{oc} =$	2.562	V
$\eta =$	11.20	%
FF =	70.19	%
$P_{MAX} =$	15.832	W
$V_{Pmax} =$	1.963	V
$I_{Pmax} =$	8.066	A
$R_s =$	0.0	Ω
$R_p =$	66.5	Ω
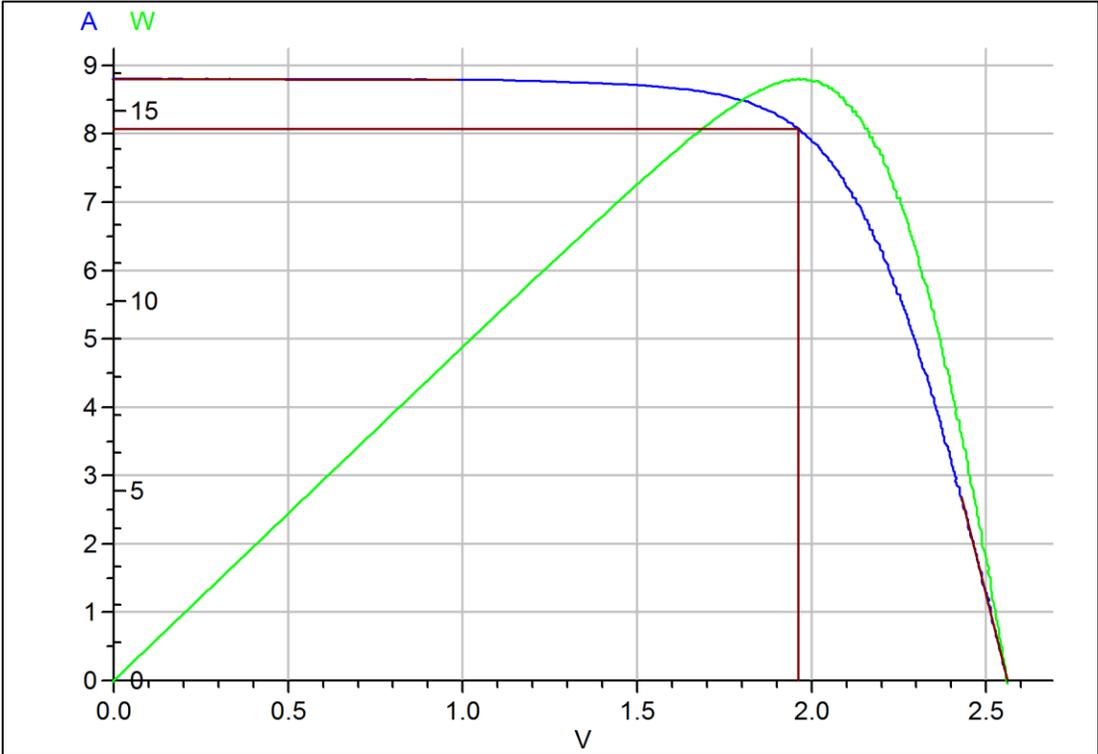
Figure 43: I-V and P-V diagrams for module no16.

The following table summarizes the basic parameters measured for above three PV panels:

Table 2: Flash test results – mono-Si, multi-Si, defective multi-Si

	no6	no20	no16
Pmax[W]	16.386	15.996	15.832
FF[%]	71.18	70.72	70.19
η[%]	11.59	11.31	11.2
Isc[A]	8.925	8.832	8.806
Voc[V]	2.579	2.561	2.562
Rs[Ω]	0	0	0
Rsh[Ω]	49.2	68.7	66.5

The following graphs show the *I-V* and *P-V* curves for the same panels (the values for plotting the I-V curves and P-V curves for PV panels no6, no16 and no20 can be found in annex [D]).
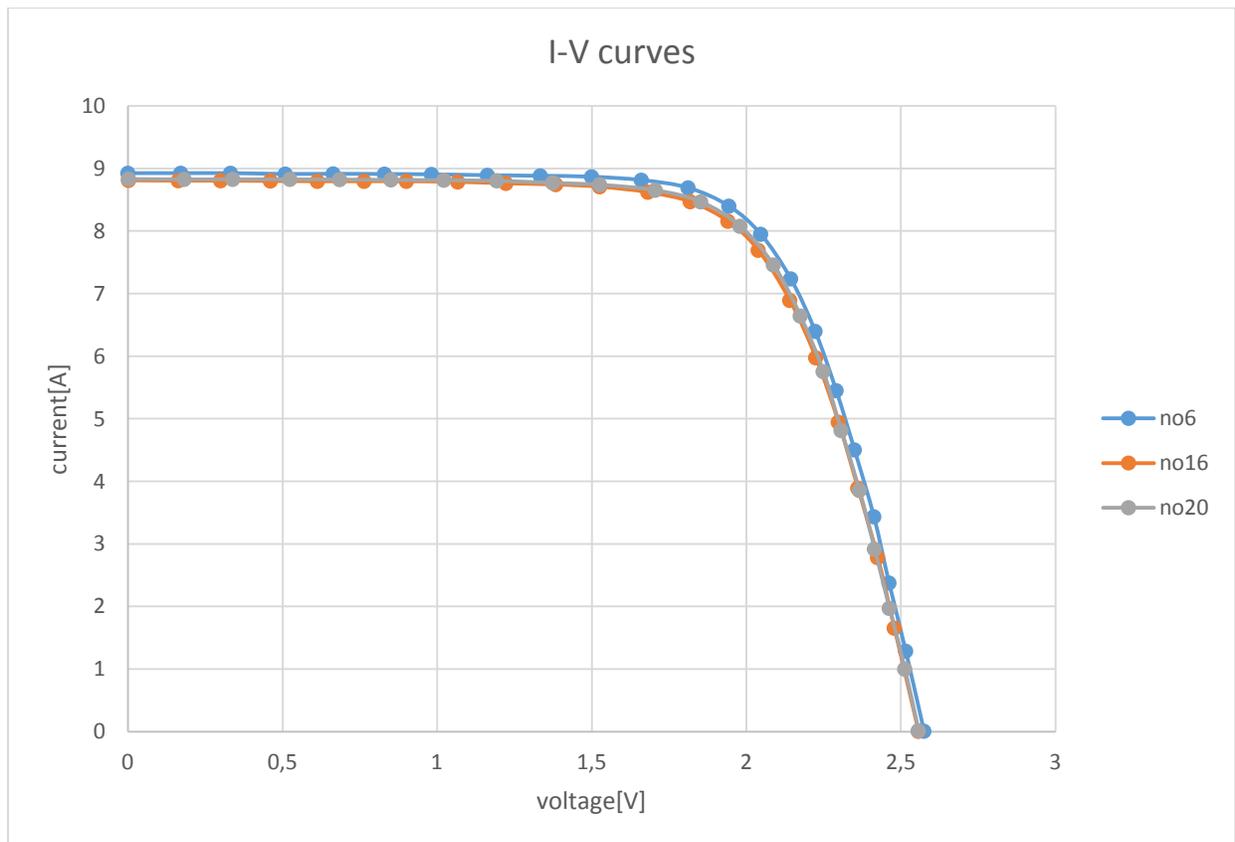
Figure 44: I-V curves for modules no6, no20, no16.
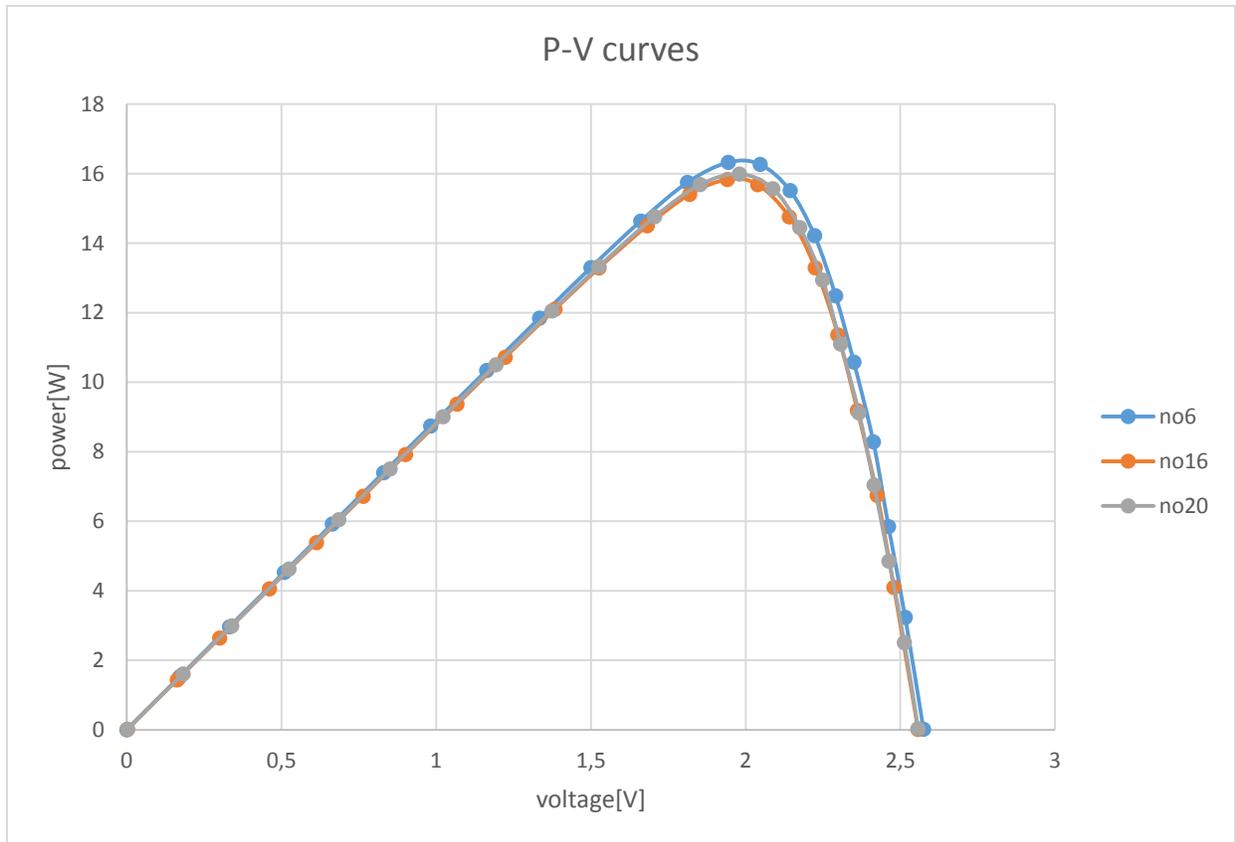
Figure 45: P-V curves for modules no6, no20, no16.

According to the measured values and the graphs, mono-crystalline panel no6 has better performance than the compared multi-crystalline panels. More specifically, no6 has bigger power output and better efficiency than no16 and no20. Comparing the two multi-crystalline panels, no20 has little more bigger output and better efficiency than no20 but it is not a surprise, as no16 has a defective cell according to previous measurement using electroluminescence method test. But the difference between these two curves is almost non-observable.

4.3.3 Impedance spectroscopy

After measuring the 18 PV modules, we choose 3 of them: one mono-crystalline (no6), one multi-crystalline (no20) and one multi-crystalline that seems to be defective (no16).

After measuring the dynamic parameters for mono-crystalline (no6), multi-crystalline (no20) and multi-crystalline (no16) in a range of frequency from 20 Hz to 80 kHz and plotting the real and imaginary values $R(\omega)$ and $X(\omega)$ we measured on complex plane in dependence of frequency, we take the impedance spectrum of the system (cole-cole plots): (the values can be found in annex[G]):
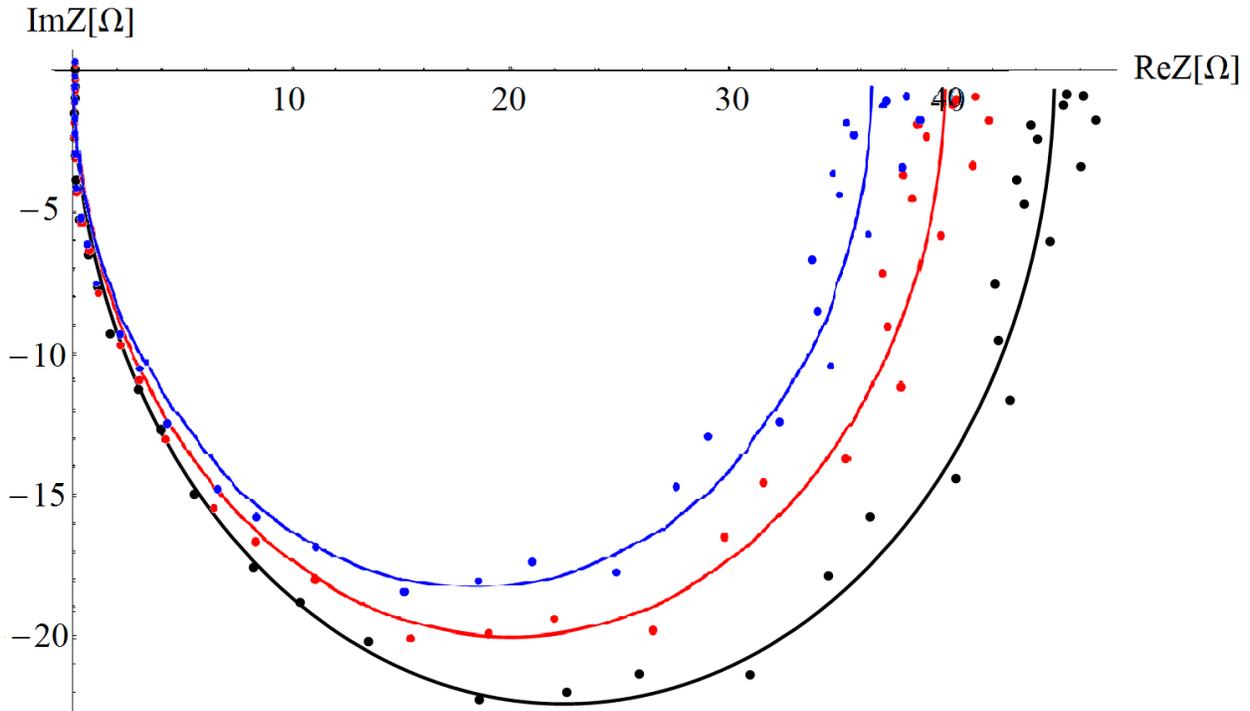
Figure 46: The cole-cole plots for PV modules no6 (black), no20 (red) and no16 (blue).

According to theory measuring the dynamic impedance of solar modules and plot them in the complex plane, it is possible to understand about the quality of the module. In our case and according to the above cole-cole plots, module no16 is the lowest quality module, no6 is the highest quality module and module no20 has a quality almost between no6 and no20. Despite the fact that only impedance characteristics were measured in this measurement, after making the plots, we can conclude that no16 has the lowest efficiency and the lowest *FF,* no6 has the best efficiency and the biggest *FF* and no20 has efficiency and *FF* almost between no16 and no6.

5 CONCLUSION

The needs for electricity are increased day to day, the oil fuels are becoming more and more expensive and the environmental pollution make scientists and researchers try to find or improve existing alternative ways for energy sources. Renewable sources are one of these alternatives because of their low CO_2 pollution and the decrease of their cost the last years. More specifically, photovoltaic technology is becoming more and more popular because of its many applications in everyday life. This is the reason why scientists and researchers aim to improve the efficiency of the PV cells and make them more reliable.

Many materials are used for making PV cells but Silicon seems to be the most popular among others as it dominates the market. Either mono-crystalline or multi-crystalline, they are tested with many different methods or techniques trying to improve these parameters that can make them more efficient. Impedance spectroscopy is one of these methods that examines the dynamic parameters of a PV cell. It is the complex impedance behavior of the PV systems that make researchers pay so much attention to detailed analysis of their AC parameters. Changes in temperature or irradiance can affect the real or imaginary part of the system and the measurement of some or all impedance related functions in a large range of frequencies from 20 Hz to 80000 Hz can give much information about the quality or the operating condition of the cell. A pure sinusoidal voltage is applied to the system under test and plotting the real and imaginary values $R(\omega)$ and $X(\omega)$ in dependence on frequency can conclude the impedance spectrum which can help us calculate other equivalent circuit parameters. Even if the static characteristics of the system are unknown, impedance spectroscopy can give all these information required to evaluate the quality of the cell.

Another measurement technique that helps investigate possible breakages or cracks on a cell is electroluminescence. Electroluminescence is a photographic technique that uses special kinds of cameras operating in high speed and big sensitivity. During measurement the cell emit infrared light and the camera captures the surface of the cell in less than 1 s. Pictures that are taken show defects or breakages of the cell that it is impossible to be seen by naked eye. Temperature in this kind of measurement plays important role as increase of temperature can change the EL intensity contrast giving more possibilities for researchers to investigate more thoroughly the cell's condition.

A third kind of measurement technique that is widely used for testing the quality and performance of PV modules is flash tests. Using flash testers, the PV module is tested in a dark tunnel where a flash emits a high light intensity which lasts for few milliseconds. In this milliseconds, the I-V curve of the module is recorded using some relative computer software and the basic parameters like V_{OC}, I_{SC}, P_{MAX}, FF, R_S, R_{SH} and η are recorded as well.

There were 9 monocrystalline and 9 multicrystalline PV modules measured using EL testing, flash tests and impedance spectroscopy. From measured PV modules the representatives from both groups were chosen for comparison. According to EL measurement also module number 16 which showed defect at one cell was chosen for further comparison.

From the comparison of flash tests, there was found that monocrystalline PV modules have better performance than the multicrystalline ones. Also small difference between good and defective multicrystalline PV module was observed. Looking in detail the table 2, we confirm that no16 has indeed the lowest values of P_{MAX}, efficiency and *FF* as it seemed from the impedance spectroscopy and electroluminescence measurements. No6 has the biggest values and no20 is between no6 and no20. However the differences are quite small despite the fact that no16 has a defected part on the down-right side of the module but it does not affect the operation of the module. There was no deformation of the *I-V* curve (which is typical for crack defects) observed.

The impedance spectroscopy method showed more obviously the differences between two technologies and also between good and defective PV module. This method is probably more sensitive to initializing defects than flash test.

Applying diagnostic tests on PV modules using these techniques or others, we can detect possible deviations against specifications, we can check the performance against the performance specifications and find the cause for these deviations. The consequences from such deviations can cause problems to PV systems decreasing the output power. Combining diagnostic measurement techniques, scientists have better understanding of the way PV cells and modules behave in different environment condition, helping them build more efficient and stable PV systems.

6 REFERENCES:

[1]   IRENA (2015), *Renewable Power Generation Costs in 2014*

[2]   Gray, Jeffery L. The Physics of the Solar Cell. A. Luque a S. Hegedus. *Handbook of Photovoltaic Science and Engineering*. Chichester : John Wiley & Sons, Ltd., 2003, 3.

[3]   HABERLIN, Heinrich a Swapnil DUBEY. 2012. *Photovoltaics: system design and practice*. Editor Frank Kreith, D Goswami. Chichester, West Sussex: John Wiley, xxix, 701 p. Mechanical engineering series (CRC Press). ISBN 978-111-9992-851.

[4]   HOLOVSKÝ, Jakub. *Diagnostic, tests and characterization methods in PV* [online presentation]. 2015 [cited 2015-05-14]. Available at: http://pasan.feld.cvut.cz/en/ae1b13svs/index.php

[5]   IBRAHIM, A., Athapol KITIYANAN, Takashi FUYUKI a Ayumi TANI. 2006. *Analysis of Electrical Characteristics of Photovoltaic Single Crystal Silicon Solar Cells at Outdoor Measurements*. Editor Frank Kreith, D Goswami. New York: Nova Science Publishers, ix, 256 p. DOI 10.4236/sgre.2011.22020.

[6]   Taylor, N. (Ed.): *Guidelinesfor PV PowerMeasurement in Industry*, Italy: EuropeanComission, Joint Research Centre, Institute forEnergy. 2010-04. Cite 2011. ISBN: 978-92-79-15780-6.

[7]   EPIA. *GLOBAL MARKET OUTLOOK: For Photovoltaics 2014-2018* [online]. 2015 [cit. 2015-05-20]. ISBN 9789082228403. Available at: http://www.epia.org/news/publications/

[8]   GREEN, Martin A., Keith EMERY, Yoshihiro HISHIKAWA, Wilhelm WARTA a Ewan D. DUNLOP. 2010. *Solar cell efficiency tables (Version 45): the Earthscan expert handbook for planning, design, and installation*. Editor Frank Kreith, D Goswami. Washington, DC: Earthscan, xiv, 232 p. DOI 10.1002/pip.2573.

[9]   TIWARI, G a Swapnil DUBEY. 2010. *Fundamentals of photovoltaic modules and their applications*. Editor Frank Kreith, D Goswami. Cambridge: Royal Society of Chemistry, xx, 402 p. Mechanical engineering series (CRC Press). ISBN 18-497-3020-2

[10]   CHEVNIDHYA, D., K. KIRTIKARA a C. JIVACATE Dynamic Impedance Characterization of Solar Cells and PV Modules Based on Frequency and Time Domain Analyses. *Trends In Solar Energy Research*. Hough, T.P. New York: Nova Science Publishers, 2006, s. 21-45. ISBN 1-59454-866-8; LCCN: 2005034740.

[11]   ABDULLAH, K. Al, A. ALLOUSH, Takashi SALAME a Ayumi TANI. 2006. *Investigation of the Monocrystalline Silicon Solar Cell Physical Behavior after Thermal Stress by AC Impedance Spectra*. Editor Frank Kreith, D Goswami. New York: Nova Science Publishers, ix, 256 p. DOI 10.1016/j.egypro.2014.06.004.

[12]   Impedance spectroscopy: A general introduction and application to dye-sensitized solar cells

[13]   FUYUKI, Takashi, Athapol KITIYANAN, Takashi FUYUKI a Ayumi TANI. *Photographic diagnosis of crystalline silicon solar cells utilizing electroluminescence*. Editor Frank Kreith, D Goswami. ISBN 10.1007/978-1-4419-9792-0_27.

[14] KEOGH, W, A. CUEVAS, Takashi FUYUKI a Ayumi TANI. 2006. *Simple flashlamp I-V testing of solar cells*. Editor Frank Kreith, D Goswami. New York: Nova Science Publishers, ix, 256 p. DOI 10.1109/pvsc.1997.654063.

[15] KEOGH, W, Athapol KITIYANAN, Takashi FUYUKI a Ayumi TANI. 2006. *Constant voltage I–V curve flash tester for solar cells*. Editor Frank Kreith, D Goswami. New York: Nova Science Publishers, ix, 256 p. ISBN 10.1016/j.solmat.2003.11.001.

ANNEXES:

1 **[A] The characteristics of the PV modules were used for our measurements:**

2 [B]The pictures of the electroluminescence measurement:

Mono-crystalline:

(no1)	(no3)	(no4)
(no5)	(no7)	(no8)

(no9)	(no10)

Multi-crystalline:
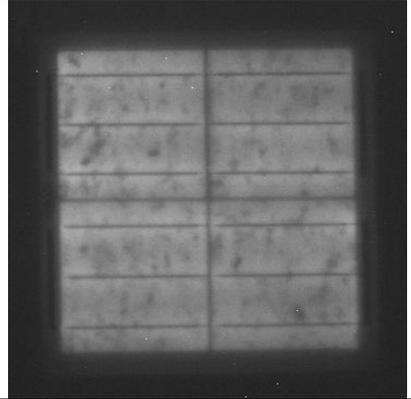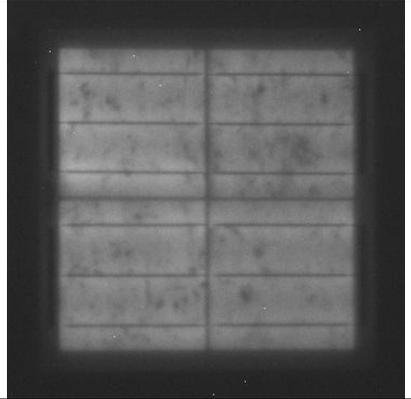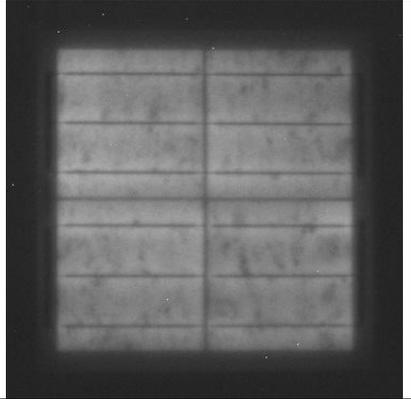
(no11)	(no12)	(no13)
(no14)	(no17)	(no18)
	(no19)	
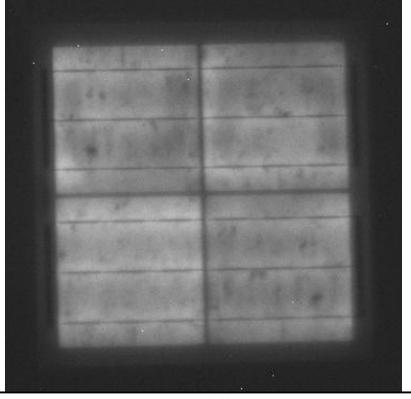
3 [C]The results from FlashTest measurement:

Mono-crystalline:
Measurement of the module number 1

Producer:	Phonosolar
Type:	PS15M
Serial number:	1
Designation in LPVS:	
Date of the measurement:	04-05-15
Actual temperature:	23.9 °C
The values are converted to the temperature:	25.0 °C
$G =$	1.0 kW/m2
$I_{sc} =$	8.910 A
$V_{oc} =$	2.547 V
$\eta =$	11.36 %
FF =	70.74 %
$P_{MAX} =$	16.056 W
$V_{Pmax} =$	1.945 V
$I_{Pmax} =$	8.253 A
$R_s =$	0.0 Ω
$R_p =$	51.2 Ω
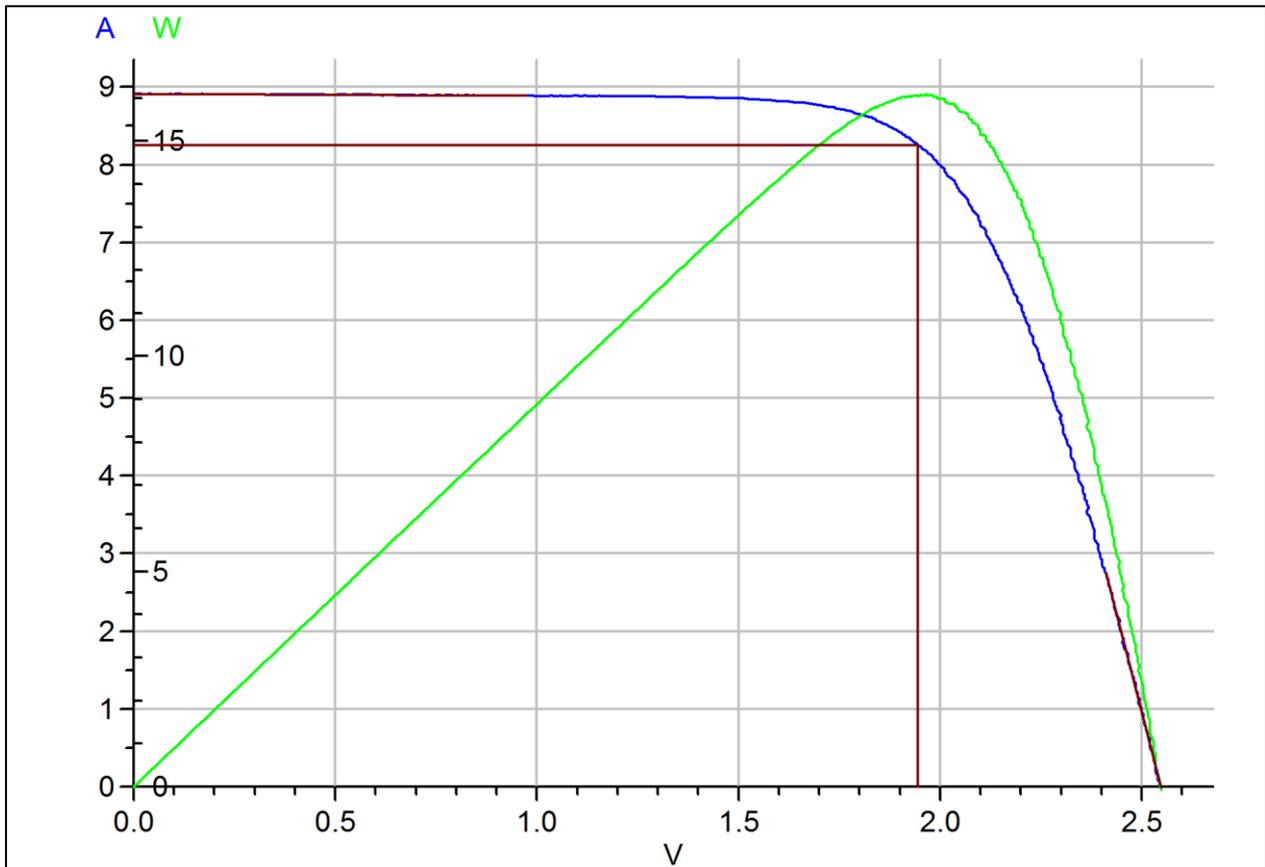
Measurement of the module number 3

Producer:	Phonosolar
Type:	PS15M
Serial number:	3
Designation in LPVS:	
Date of the measurement:	04-05-15
Actual temperature:	23.9 °C
The values are converted to the temperature:	25.0 °C
$G =$	1.0 kW/m2
$I_{sc} =$	8.950 A
$V_{oc} =$	2.554 V
$\eta =$	11.49 %
FF =	71.06 %
$P_{MAX} =$	16.243 W
$V_{Pmax} =$	1.960 V
$I_{Pmax} =$	8.288 A
$R_s =$	0.0 Ω
$R_p =$	46.1 Ω

V
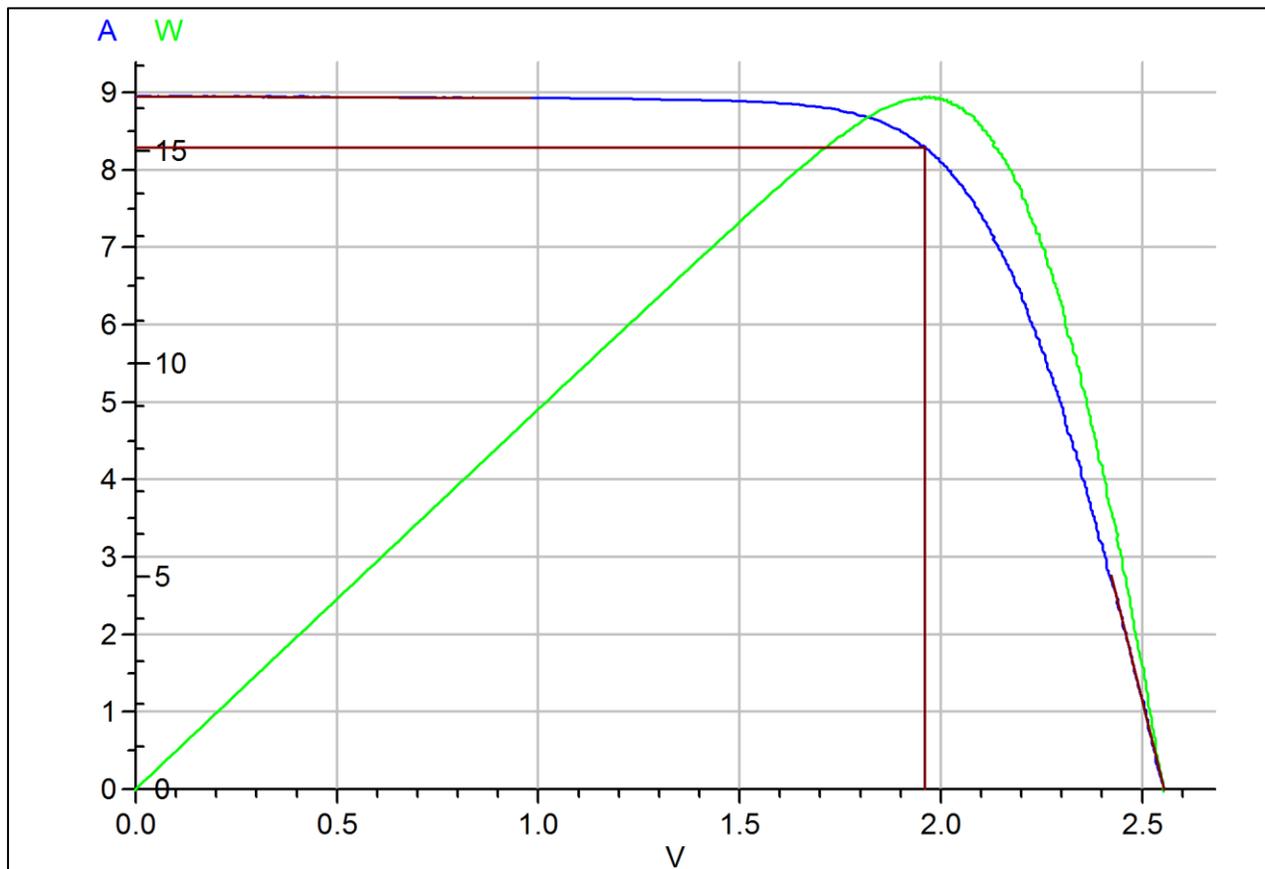
Measurement of the module number 4

Producer:	Phonosolar
Type:	PS15M
Serial number:	4
Designation in LPVS:	
Date of the measurement:	04-05-15
Actual temperature:	24.1 °C
The values are converted to the temperature:	25.0 °C
$G =$	1.0 kW/m2
$I_{sc} =$	8.907 A
$V_{oc} =$	2.563 V
$\eta =$	11.47 %
FF $=$	71.07 %
$P_{MAX} =$	16.223 W
$V_{Pmax} =$	1.967 V
$I_{Pmax} =$	8.249 A
$R_s =$	0.0 Ω
$R_p =$	65.6 Ω

Measurement of the module number 5

Producer:	Phonosolar
Type:	PS15M
Serial number:	5
Designation in LPVS:	
Date of the measurement:	04-05-15
Actual temperature:	24.0 °C
The values are converted to the temperature:	25.0 °C
$G =$	1.0 kW/m2
$I_{sc} =$	8.971 A
$V_{oc} =$	2.574 V
$\eta =$	11.67 %
FF $=$	71.43 %
$P_{MAX} =$	16.495 W
$V_{Pmax} =$	1.988 V
$I_{Pmax} =$	8.296 A
$R_s =$	0.0 Ω
$R_p =$	61.3 Ω
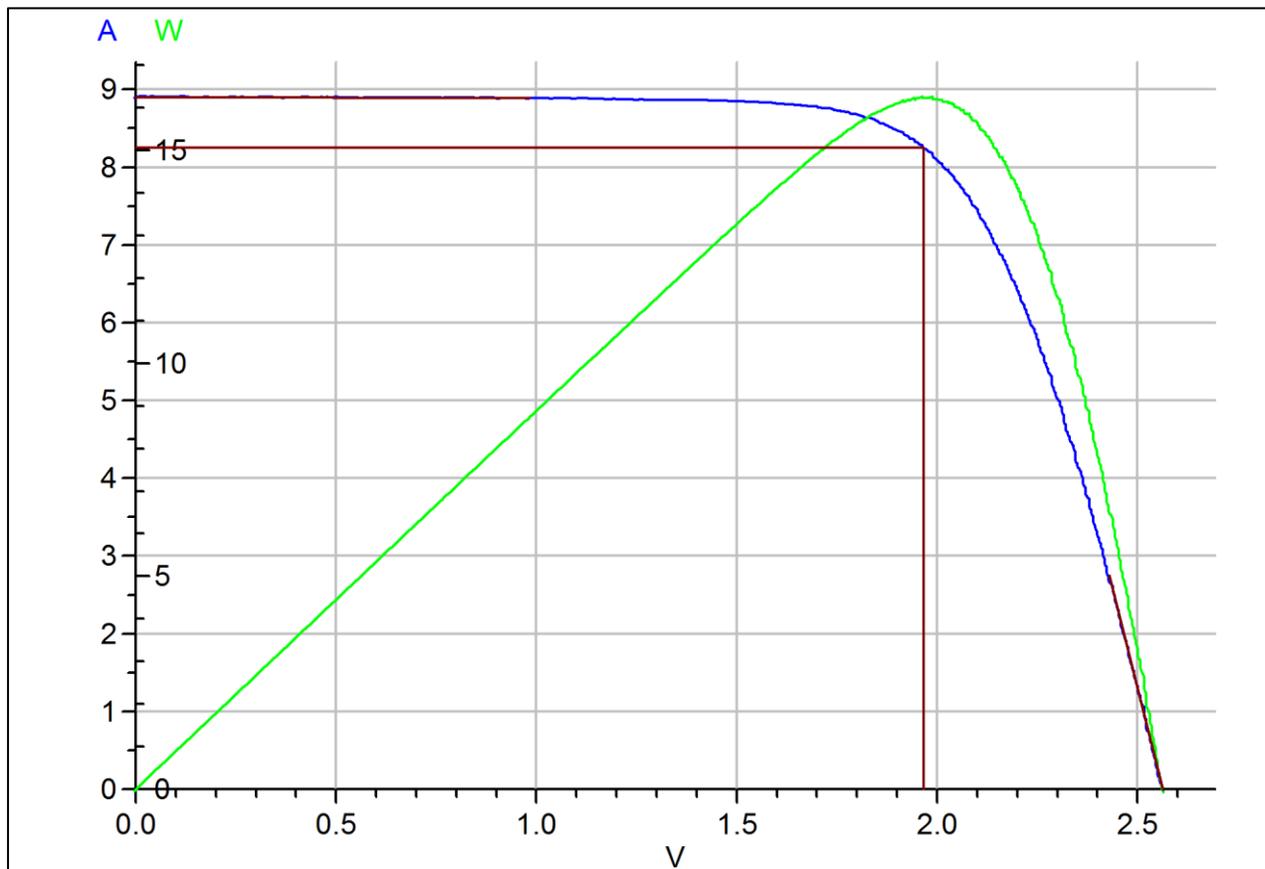
Measurement of the module number 7

Producer:	Phonosolar
Type:	PS15M
Serial number:	7
Designation in LPVS:	
Date of the measurement:	04-05-15
Actual temperature:	23.9 °C
The values are converted to the temperature:	25.0 °C
$G =$	1.0 kW/m2
$I_{sc} =$	8.983 A
$V_{oc} =$	2.567 V
$\eta =$	11.64 %
FF $=$	71.34 %
$P_{MAX} =$	16.454 W
$V_{Pmax} =$	1.978 V
$I_{Pmax} =$	8.319 A
$R_s =$	0.0 Ω
$R_p =$	59.2 Ω
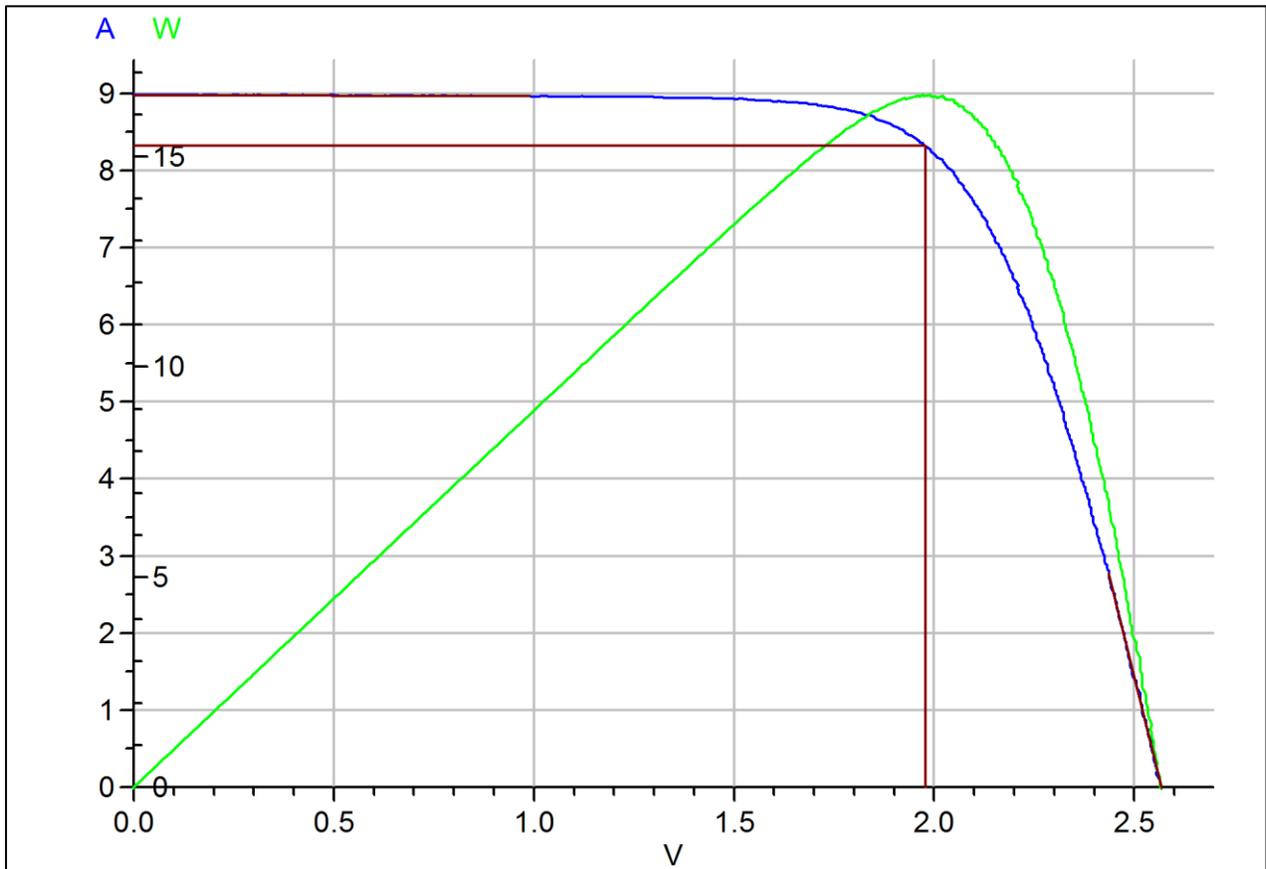
Measurement of the module number 8

Producer:	Phonosolar
Type:	PS15M
Serial number:	8
Designation in LPVS:	
Date of the measurement:	04-05-15
Actual temperature:	24.0 °C
The values are converted to the temperature:	25.0 °C
$G =$	1.0 kW/m2
$I_{sc} =$	8.958 A
$V_{oc} =$	2.576 V
$\eta =$	11.68 %
FF $=$	71.53 %
$P_{MAX} =$	16.509 W
$V_{Pmax} =$	1.989 V
$I_{Pmax} =$	8.299 A
$R_s =$	0.0 Ω
$R_p =$	94.5 Ω
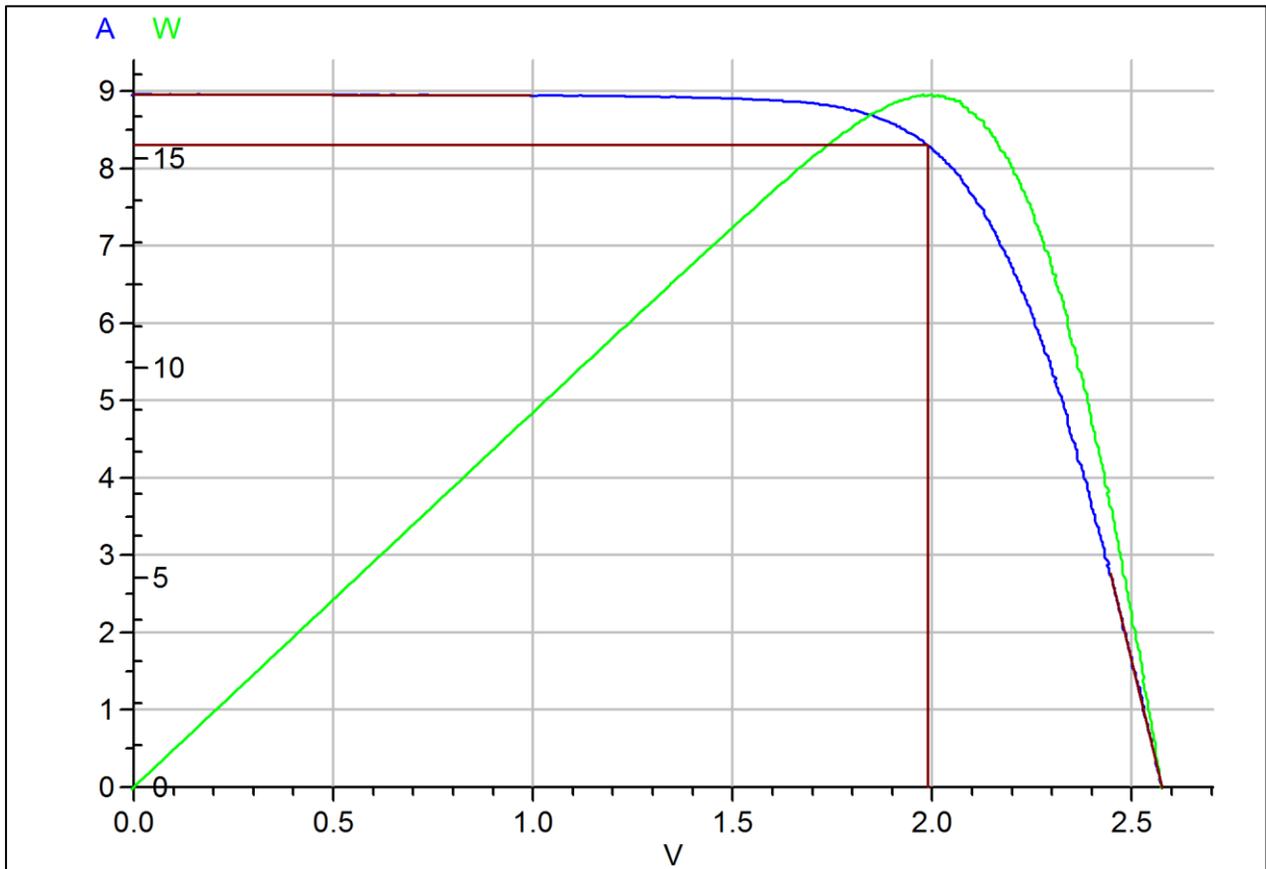
Measurement of the module number 9

Producer:	Phonosolar
Type:	PS15M
Serial number:	9
Designation in LPVS:	
Date of the measurement:	04-05-15
Actual temperature:	24.0 °C
The values are converted to the temperature:	25.0 °C
$G =$	1.0 kW/m2
$I_{sc} =$	8.946 A
$V_{oc} =$	2.558 V
$\eta =$	11.47 %
$FF =$	70.85 %
$P_{MAX} =$	16.212 W
$V_{Pmax} =$	1.961 V
$I_{Pmax} =$	8.269 A
$R_s =$	0.0 Ω
$R_p =$	58.0 Ω
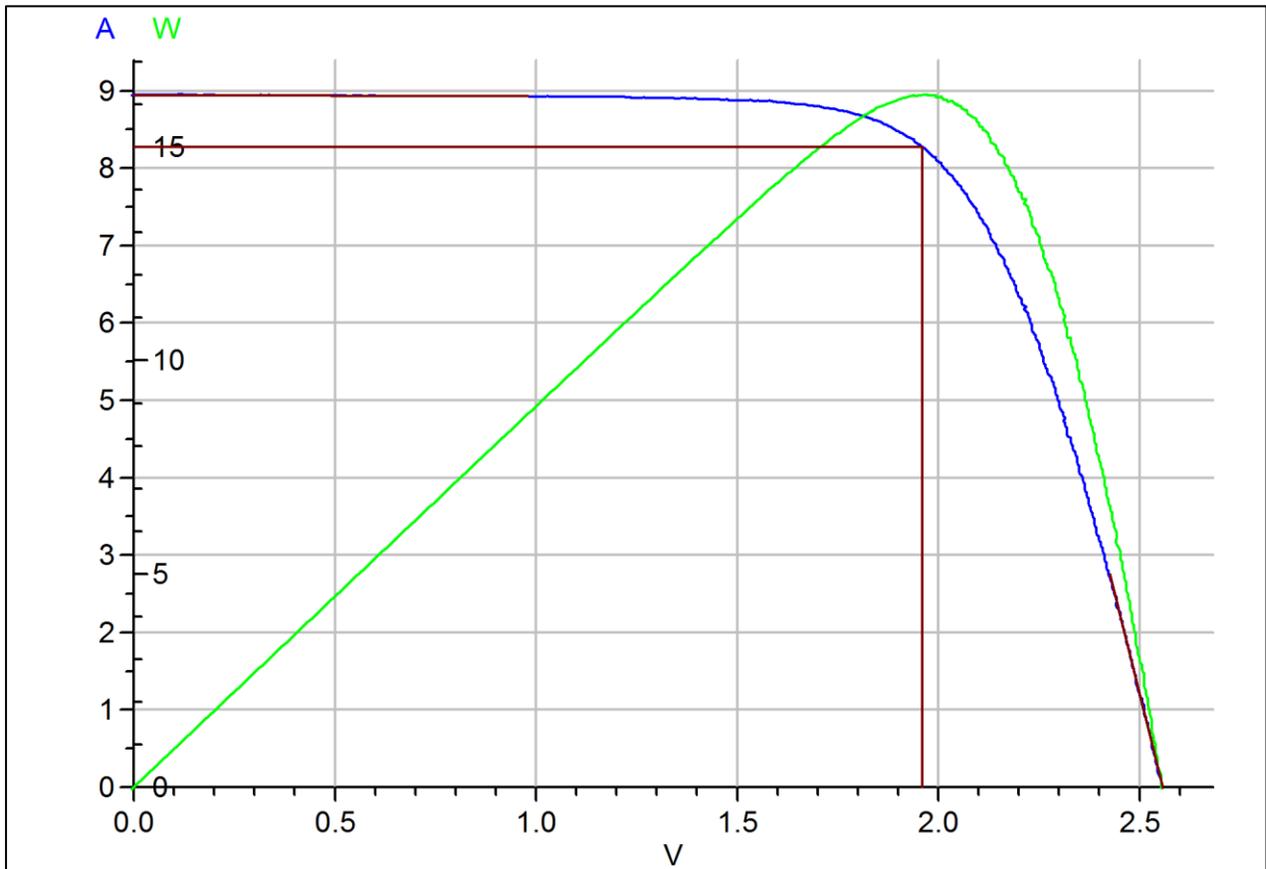
Measurement of the module number 10

Producer:	Phonosolar
Type:	PS15M
Serial number:	10
Designation in LPVS:	
Date of the measurement:	04-05-15
Actual temperature:	24.0 °C
The values are converted to the temperature:	25.0 °C
$G =$	1.0 kW/m2
$I_{sc} =$	8.963 A
$V_{oc} =$	2.566 V
$\eta =$	11.61 %
FF =	71.38 %
$P_{MAX} =$	16.415 W
$V_{Pmax} =$	1.978 V
$I_{Pmax} =$	8.301 A
$R_s =$	0.0 Ω
$R_p =$	57.2 Ω
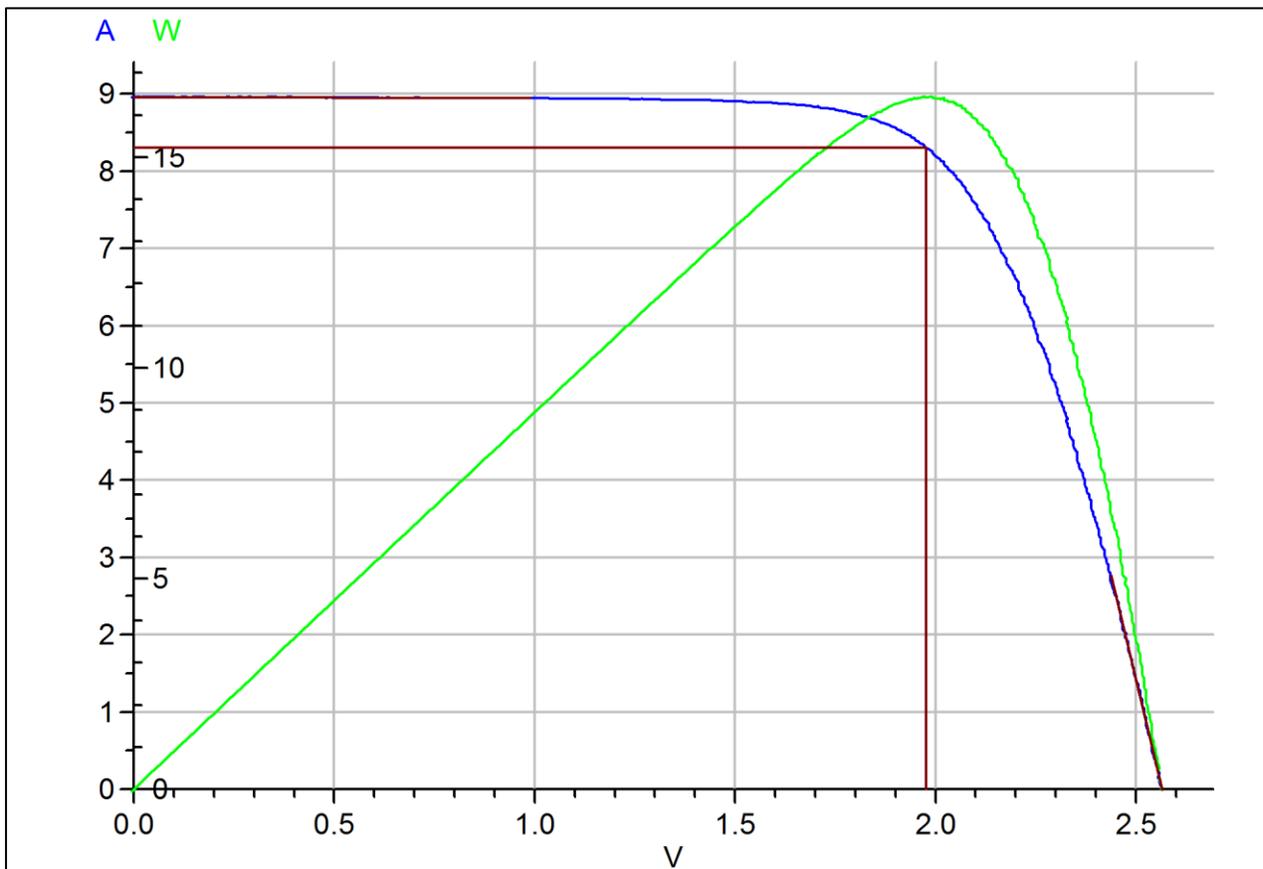
Multi-crystalline:

Measurement of the module number 11

Producer:	Phonosolar	
Type:	PS15P	
Serial number:	11	
Designation in LPVS:		
Date of the measurement:	04-05-15	
Actual temperature:	23.7	°C
The values are converted to the temperature:	25.0	°C
$G =$	1.0	kW/m2
$I_{sc} =$	8.835	A
$V_{oc} =$	2.523	V
$\eta =$	11.22	%
FF =	71.14	%
$P_{MAX} =$	15.858	W
$V_{Pmax} =$	1.936	V
$I_{Pmax} =$	8.193	A
$R_s =$	0.0	Ω
$R_p =$	77.1	Ω
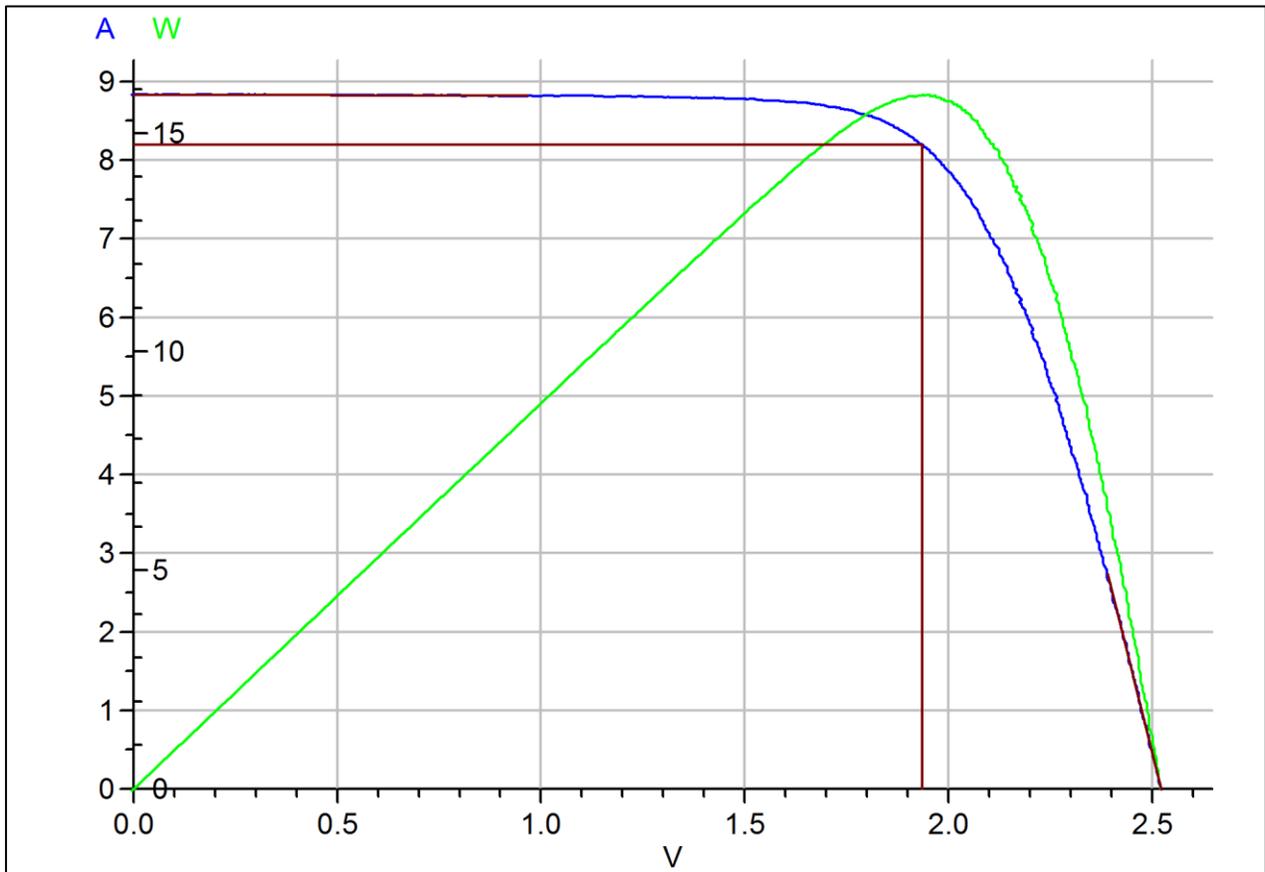
Measurement of the module number 12

Producer:	Phonosolar
Type:	PS15P
Serial number:	12
Designation in LPVS:	
Date of the measurement:	04-05-15
Actual temperature:	23.7 °C
The values are converted to the temperature:	25.0 °C
$G =$	1.0 kW/m2
$I_{sc} =$	8.818 A
$V_{oc} =$	2.514 V
$\eta =$	11.14 %
$FF =$	71.07 %
$P_{MAX} =$	15.755 W
$V_{Pmax} =$	1.926 V
$I_{Pmax} =$	8.180 A
$R_s =$	0.0 Ω
$R_p =$	58.0 Ω
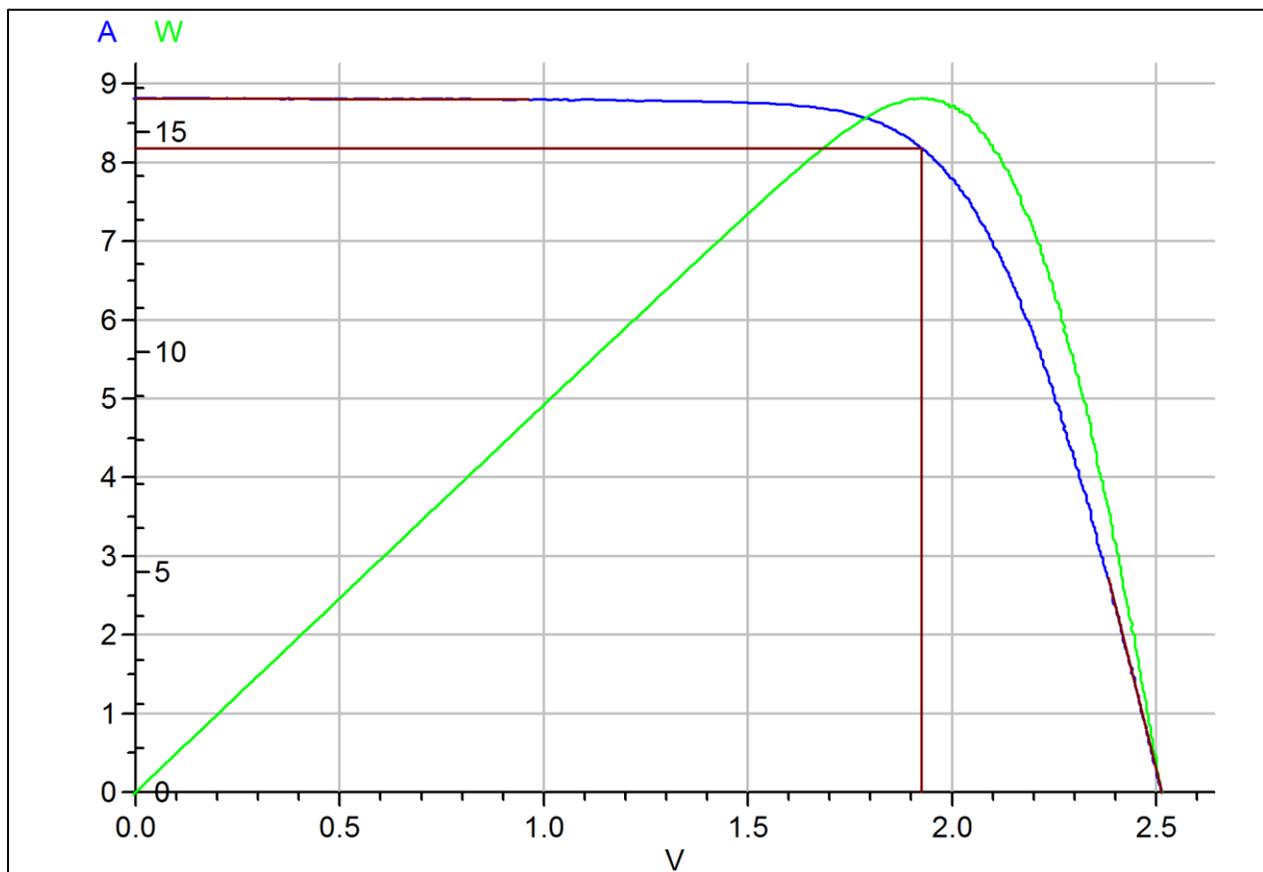
Measurement of the module number 13

Producer:	Phonosolar
Type:	PS15P
Serial number:	13
Designation in LPVS:	
Date of the measurement:	04-05-15
Actual temperature:	23.8 °C
The values are converted to the temperature:	25.0 °C
$G =$	1.0 kW/m2
$I_{sc} =$	8.816 A
$V_{oc} =$	2.537 V
$\eta =$	11.31 %
$FF =$	71.53 %
$P_{MAX} =$	15.996 W
$V_{Pmax} =$	1.952 V
$I_{Pmax} =$	8.195 A
$R_s =$	0.0 Ω
$R_p =$	65.9 Ω
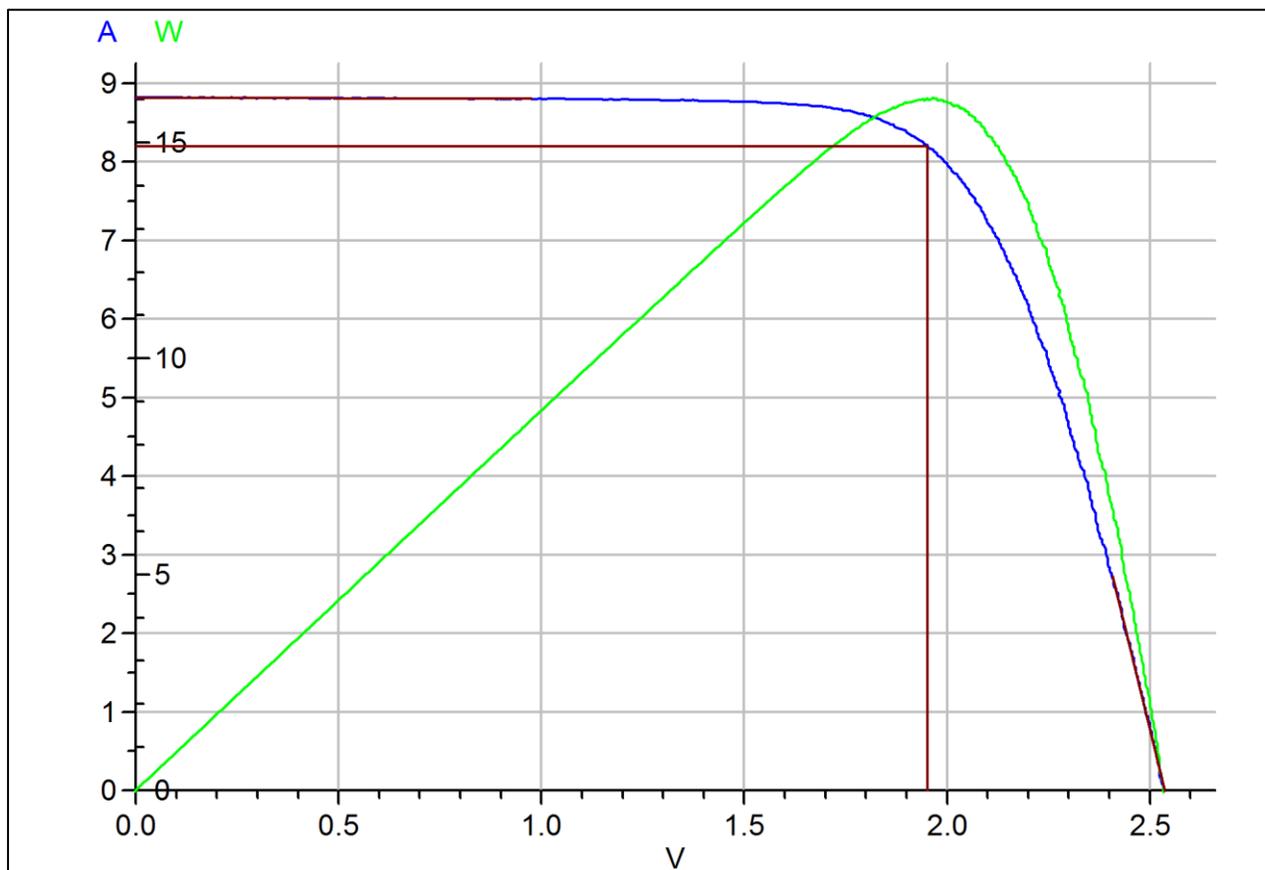
Measurement of the module number 14

Producer:	Phonosolar
Type:	PS15P
Serial number:	14
Designation in LPVS:	
Date of the measurement:	04-05-15
Actual temperature:	23.8 °C
The values are converted to the temperature:	25.0 °C
$G =$	1.0 kW/m2
$I_{sc} =$	8.833 A
$V_{oc} =$	2.565 V
$\eta =$	11.38 %
$FF =$	71.04 %
$P_{MAX} =$	16.092 W
$V_{Pmax} =$	1.974 V
$I_{Pmax} =$	8.153 A
$R_s =$	0.0 Ω
$R_p =$	85.8 Ω
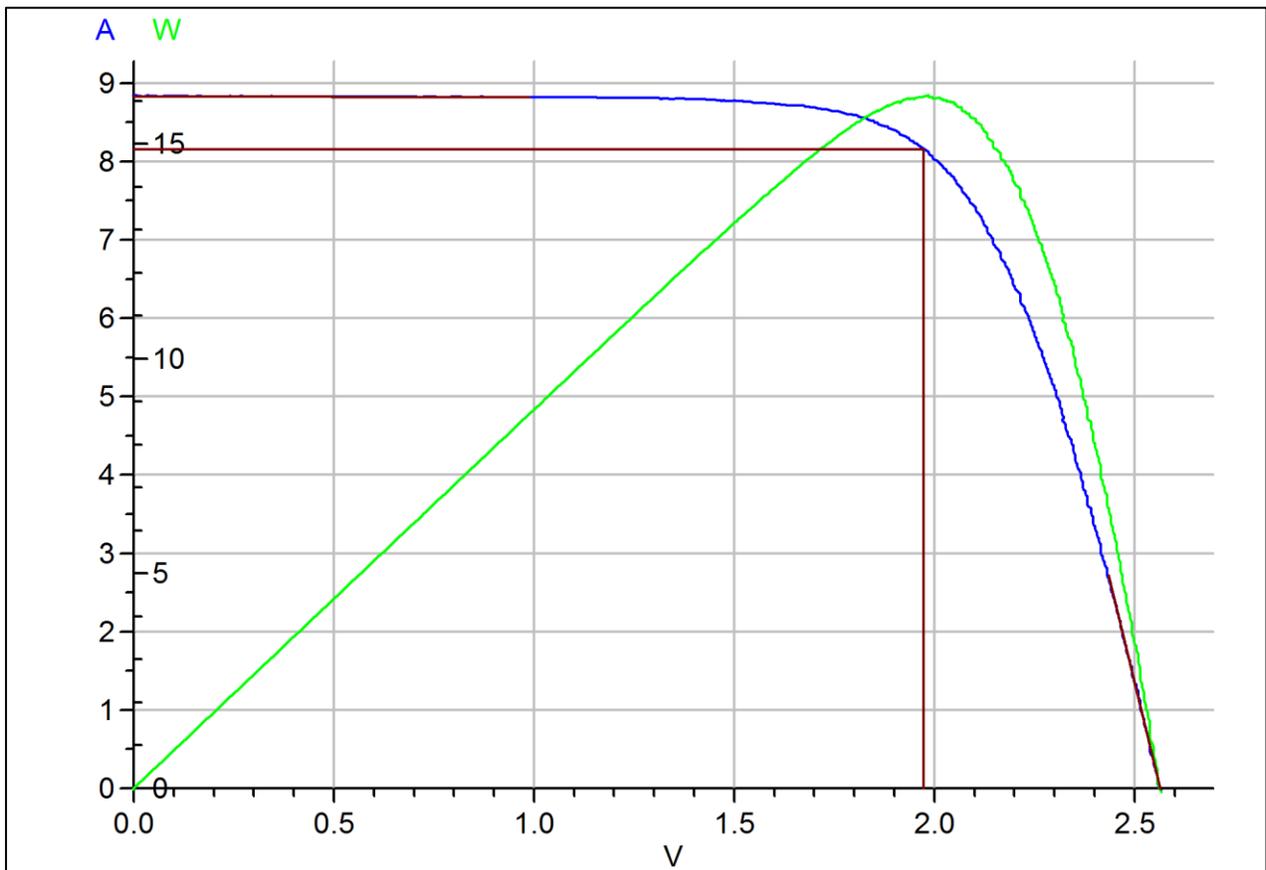
Measurement of the module number 17

|	
Producer:	Phonosolar
Type:	PS15P
Serial number:	17
Designation in LPVS:	
Date of the measurement:	04-05-15
Actual temperature:	23.8 °C
The values are converted to the temperature:	25.0 °C
$G =$	1.0 kW/m2
$I_{sc} =$	8.803 A
$V_{oc} =$	2.534 V
$\eta =$	11.25 %
$FF =$	71.29 %
$P_{MAX} =$	15.905 W
$V_{Pmax} =$	1.942 V
$I_{Pmax} =$	8.191 A
$R_s =$	0.0 Ω
$R_p =$	102.1 Ω
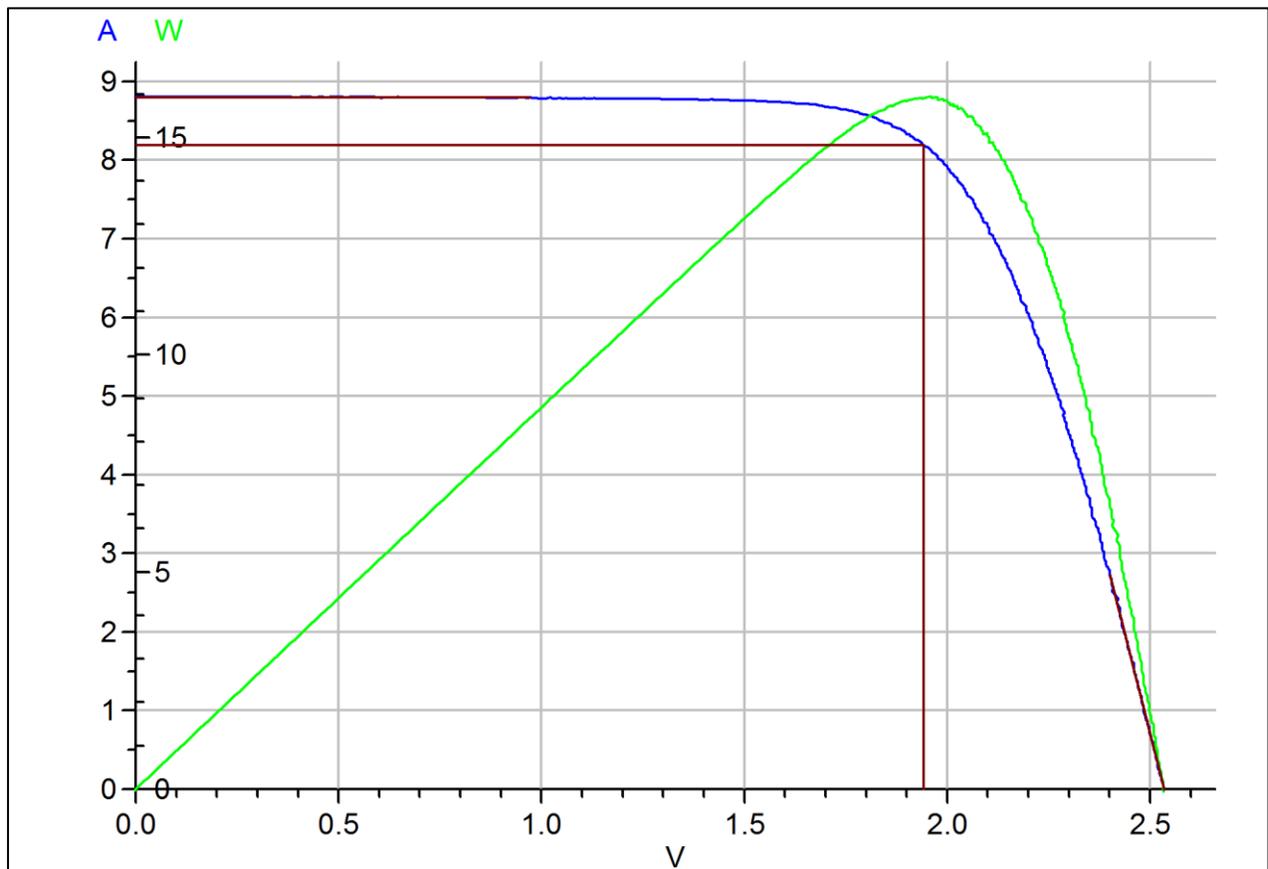
# Measurement of the module number 18

Producer: Phonosolar
Type: PS15P
Serial number: 18
Designation in LPVS:
Date of the measurement: 04-05-15
Actual temperature: 23.6 °C
The values are converted to the temperature: 25.0 °C
$G =$ 1.0 kW/m2
$I_{sc} =$ 8.868 A
$V_{oc} =$ 2.505 V
$\eta =$ 11.10 %
FF = 70.63 %
$P_{MAX} =$ 15.691 W
$V_{Pmax} =$ 1.909 V
$I_{Pmax} =$ 8.218 A
$R_s =$ 0.0 Ω
$R_p =$ 50.3 Ω
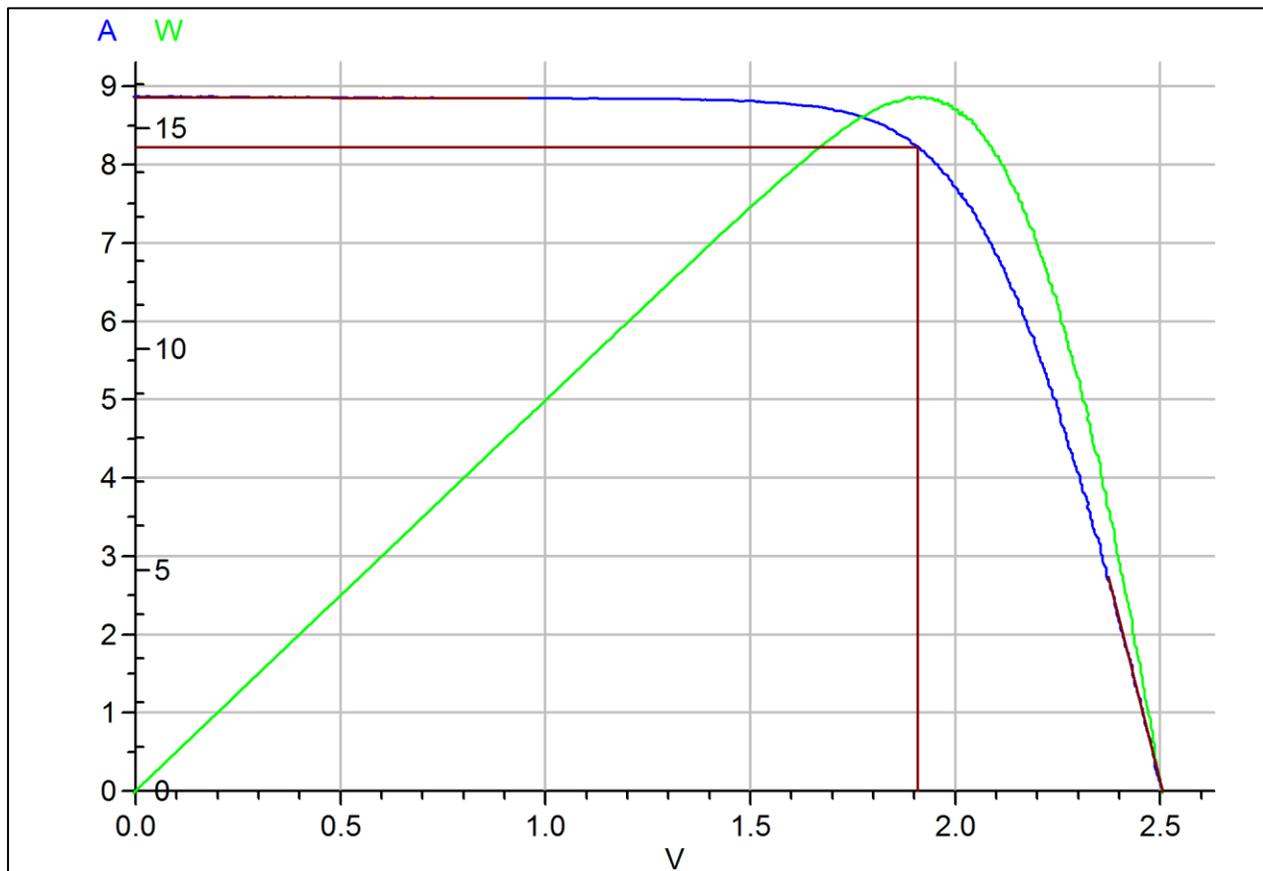
Measurement of the module number 19

Producer:	Phonosolar
Type:	PS15P
Serial number:	19
Designation in LPVS:	
Date of the measurement:	04-05-15
Actual temperature:	23.8 °C
The values are converted to the temperature:	25.0 °C
$G =$	1.0 kW/m2
$I_{sc} =$	8.795 A
$V_{oc} =$	2.545 V
$\eta =$	11.06 %
$FF =$	69.89 %
$P_{MAX} =$	15.641 W
$V_{Pmax} =$	1.935 V
$I_{Pmax} =$	8.084 A
$R_s =$	0.1 Ω
$R_p =$	74.1 Ω
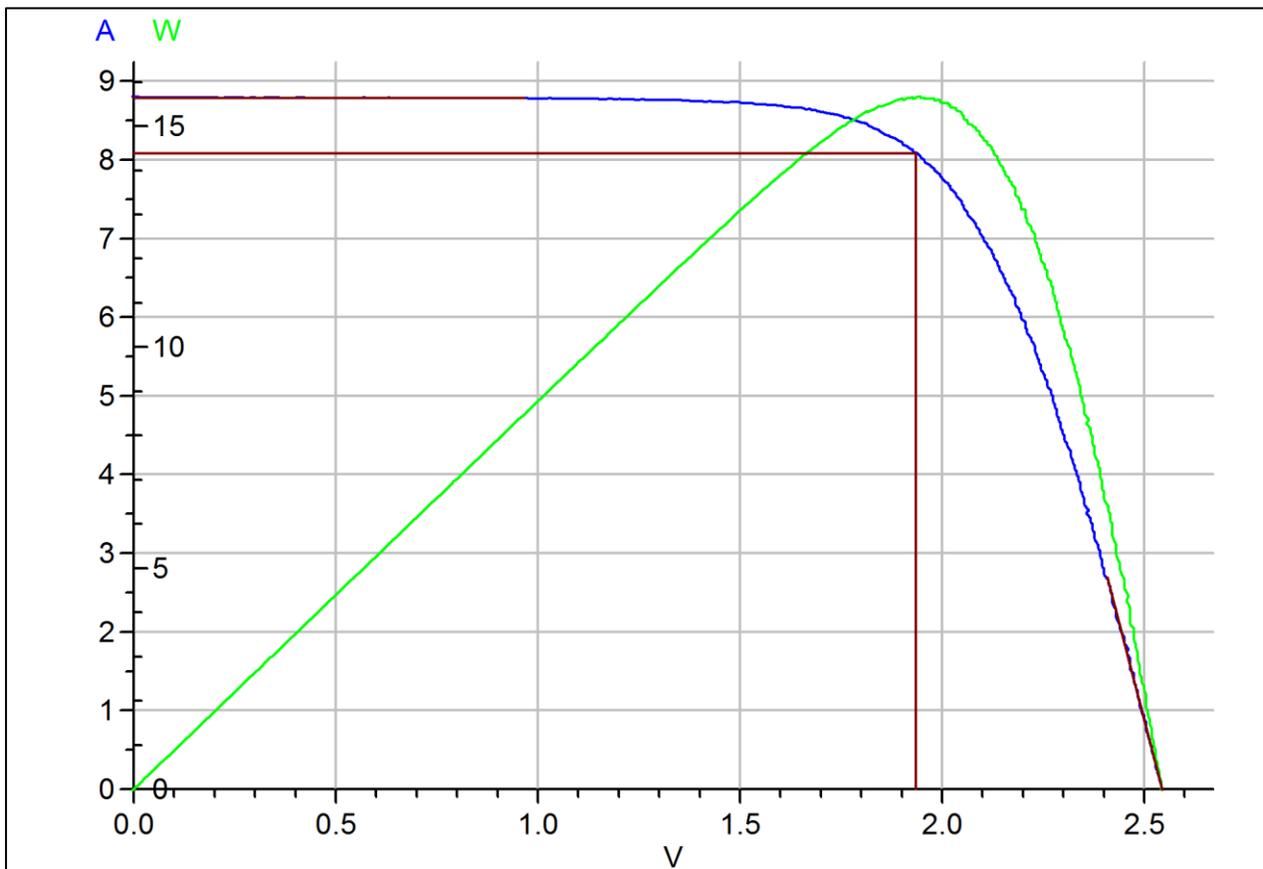
4 [D] The values for plotting the I-V curves and P-V curves for PV panels no6, no20 and no16:

	no6			no16			no20	
Voltage [V]	Current [A]	Power [W]	Voltage [V]	Current [A]	Power [W]	Voltage [V]	Current [A]	Power [W]
0	8.924	0.003	0.002	8.81	0.019	0.002	8.832	0.015
0.171	8.924	1.528	0.163	8.805	1.438	0.182	8.827	1.61
0.332	8.924	2.966	0.3	8.805	2.642	0.339	8.827	2.989
0.509	8.911	4.531	0.461	8.8	4.058	0.524	8.827	4.627
0.664	8.914	5.922	0.613	8.795	5.387	0.685	8.823	6.046
0.83	8.91	7.398	0.764	8.795	6.719	0.851	8.818	7.507
0.982	8.905	8.742	0.901	8.795	7.921	1.022	8.813	9.009
1.163	8.891	10.339	1.067	8.785	9.371	1.193	8.803	10.503
1.334	8.882	11.845	1.223	8.762	10.719	1.374	8.77	12.052
1.5	8.867	13.298	1.384	8.743	12.104	1.526	8.741	13.335
1.661	8.813	14.637	1.526	8.708	13.289	1.706	8.653	14.764
1.812	8.691	15.75	1.682	8.621	14.502	1.853	8.467	15.688
1.944	8.398	16.326	1.819	8.469	15.405	1.98	8.077	15.99
2.047	7.949	16.268	1.941	8.157	15.833	2.088	7.458	15.569
2.144	7.236	15.516	2.039	7.693	15.684	2.175	6.643	14.45
2.223	6.397	14.22	2.141	6.892	14.758	2.249	5.754	12.939
2.291	5.45	12.487	2.225	5.975	13.293	2.307	4.812	11.101
2.35	4.503	10.581	2.298	4.945	11.364	2.366	3.855	9.119
2.413	3.434	8.286	2.361	3.89	9.187	2.415	2.917	7.044
2.462	2.375	5.849	2.425	2.782	6.746	2.463	1.97	4.853
2.516	1.286	3.237	2.479	1.654	4.1	2.513	0.999	2.511
2.575	0.007	0.018	2.557	0.005	0.013	2.557	0.013	0.034

5 [E] The values concluding the Figure 5 and Figure 6 (the yellow highlighted lines show the P_{MPP}):

45˚C

Voltage[V]	Current[A]	Power[w]
0.496	0.000	0.000
0.495	0.042	0.021
0.493	0.066	0.033
0.492	0.090	0.044
0.490	0.112	0.055
0.489	0.146	0.071
0.473	0.366	0.173
0.453	0.563	0.255
0.441	0.641	0.283
0.418	0.730	0.305
0.370	0.834	0.309
0.280	0.870	0.244
0.173	0.871	0.151
0.067	0.883	0.059
0.000	0.880	0.000

65˚C

Voltage[V]	Current[A]	Power[w]
0.4561	0	0
0.451	0.038	0.017
0.450	0.052	0.023
0.448	0.083	0.037
0.447	0.102	0.046
0.445	0.133	0.059
0.442	0.190	0.084
0.431	0.365	0.157
0.425	0.404	0.171
0.420	0.454	0.191
0.405	0.594	0.240
0.388	0.693	0.269
0.354	0.807	0.286
0.280	0.884	0.248
0.178	0.908	0.161
0.000	0.909	0.000

85˚C

Voltage[V]	Current[A]	Power[w]
0.411	0.000	0.000
0.406	0.034	0.014
0.405	0.042	0.017
0.405	0.047	0.019
0.404	0.074	0.030
0.402	0.091	0.037
0.401	0.119	0.048
0.397	0.172	0.068
0.388	0.302	0.117
0.378	0.411	0.155
0.365	0.543	0.198
0.351	0.640	0.225
0.328	**0.763**	**0.250**
0.271	0.883	0.240
0.172	0.914	0.157
0.000	0.943	0.000

105˚C

Voltage[V]	Current[A]	Power[w]
0.367	0.000	0.000
0.367	0.030	0.011
0.362	0.037	0.013
0.361	0.067	0.024
0.360	0.082	0.030
0.355	0.153	0.054
0.347	0.268	0.093
0.339	0.367	0.124
0.328	0.484	0.159
0.316	0.625	0.198
0.262	**0.931**	**0.244**
0.178	0.964	0.172
0.000	0.967	0.000

6 [F] The values concluding the Figure 4 (the yellow highlighted lines show the P_{MPP}):

66cm		
Voltage[V]	*Current[Amps]*	*Power[W]*
0.574	0.000	0.000
0.571	0.049	0.028
0.570	0.061	0.035
0.570	0.068	0.039
0.569	0.079	0.045
0.567	0.110	0.062
0.566	0.137	0.078
0.564	0.183	0.103
0.559	0.270	0.151
0.544	0.514	0.280
0.544	0.516	0.281
0.540	0.563	0.304
0.535	0.623	0.333
0.527	0.696	0.367
0.515	0.783	0.403
0.491	0.883	0.434
0.437	0.962	0.421
0.355	0.999	0.354
0.263	1.012	0.266
0.161	1.029	0.166
0.061	1.041	0.063
0.000	1.035	0.000

61cm		
Voltage[V]	Current[Amps]	Power[W]
0.572	0.000	0.000
0.570	0.060	0.034
0.569	0.079	0.045
0.568	0.091	0.052
0.567	0.137	0.078
0.565	0.183	0.103
0.561	0.270	0.151
0.549	0.517	0.284
0.546	0.568	0.310
0.536	0.706	0.378
0.529	0.798	0.422
0.517	0.922	0.477
0.492	1.069	0.525
0.424	1.174	0.498
0.315	1.207	0.380
0.194	1.217	0.236
0.075	1.233	0.092
0.000	1.233	0.000

56cm		
Voltage[V]	Current[Amps]	Power[W]
0.577	0.000	0.000
0.574	0.061	0.035
0.573	0.079	0.045
0.572	0.111	0.063
0.570	0.185	0.105
0.567	0.273	0.155
0.557	0.525	0.292
0.554	0.577	0.320
0.551	0.641	0.353
0.548	0.721	0.395
0.542	0.821	0.445
0.533	0.955	0.509
0.519	1.133	0.587
0.484	1.352	0.654
0.382	1.479	0.565
0.239	1.507	0.360
0.091	1.522	0.138
0.000	1.520	0.000

7 [G] The values from impedance spectroscopy measurement for PV panels no6, no20, no16:

frequency(Hz)	6		20		16	
	R(Ω)	X(Ω)	R(Ω)	X(Ω)	R(Ω)	X(Ω)
20	46.15520	-0.89228	41.24470	-0.89082	38.23110	-0.89070
25	45.38010	-0.86022	40.36780	-1.04058	37.32120	-1.04692
30	45.24260	-1.24384	40.22230	-1.22107	37.16930	-1.23038
40	46.72960	-1.76703	41.85930	-1.74515	38.85140	-1.77844
50	43.74730	-1.94764	38.59050	-1.87535	35.49390	-1.86213
60	44.07650	-2.44046	38.94240	-2.32986	35.85030	-2.30296
80	46.02430	-3.41651	41.09710	-3.34107	38.01970	-3.35898
100	43.10430	-3.87187	37.92260	-3.67115	34.78740	-3.57335
120	43.46390	-4.73235	38.33230	-4.49876	35.18100	-4.36693
150	44.65000	-6.06851	39.65960	-5.84367	36.51660	-5.74363
200	42.13730	-7.55458	36.98820	-7.09673	33.82150	-6.69984
250	42.27860	-9.56633	37.22340	-9.02997	34.06550	-8.48806
300	42.81470	-11.68900	37.83200	-11.19280	34.68170	-10.50150
400	40.32810	-14.44580	35.34800	-13.65330	32.40790	-12.53190
500	36.41630	-15.78280	31.54380	-14.51260	28.99220	-13.03540
600	34.51190	-17.88110	29.80140	-16.42660	27.59180	-14.71610
800	30.93450	-21.37630	26.46940	-19.71810	24.94600	-17.80060
1000	25.86180	-21.36280	21.95650	-19.30260	21.00810	-17.43420
1200	22.56010	-22.01230	18.97290	-19.83330	18.42030	-18.11980
1500	18.56530	-22.28210	15.35070	-20.01130	15.15190	-18.59910
2000	13.48580	-20.22030	10.99980	-17.93900	11.02390	-16.91050
2500	10.37430	-18.81750	8.29023	-16.59120	8.35965	-15.82760
3000	8.23170	-17.58920	6.43767	-15.40460	6.49994	-14.80250
4000	5.52068	-15.00730	4.17872	-13.00900	4.21428	-12.57670
5000	4.01210	-12.70240	2.98066	-10.93860	2.99871	-10.59760
6000	2.99012	-11.29520	2.13862	-9.65333	2.14301	-9.36243
8000	1.69056	-9.31628	1.07833	-7.82991	1.07249	-7.58883
10000	1.12281	-7.63409	0.66915	-6.35180	0.66241	-6.14912
12000	0.68693	-6.53607	0.35724	-5.35575	0.35754	-5.17371
15000	0.29081	-5.30005	0.13919	-4.25916	0.15208	-4.10392
20000	0.12870	-3.88348	0.08022	-3.07744	0.09206	-2.95589
25000	0.08030	-2.99140	0.06649	-2.33770	0.07568	-2.23582
30000	0.07150	-2.36883	0.06471	-1.82049	0.07151	-1.73096
40000	0.07196	-1.53779	0.06780	-1.12234	0.07169	-1.04627
50000	0.07646	-0.98539	0.07339	-0.64968	0.07571	-0.57956
60000	0.08144	-0.57307	0.07951	-0.29037	0.08081	-0.22236
80000	0.09256	0.04086	0.09245	0.25751	0.09232	0.32698